JOURNAL OF PETROLOGY | VOLUME 38 | NUMBER 10 | PAGES 1391–1417 | 1997

Petrology and Geochronology of Eclogites from the Lanterman Range, Antarctica

G. DI VINCENZO[1,2]*, R. PALMERI[1], F. TALARICO[1], P. A. M. ANDRIESSEN[2] AND C. A. RICCI[1]

[1]DIPARTIMENTO DI SCIENZE DELLA TERRA, UNIVERSITÀ DI SIENA, VIA DELLE CERCHIA 3, 53100 SIENA, ITALY

[2]FACULTEIT DER AARDWETENSCHAPPEN, VRIJE UNIVERSITEIT, DE BOELELAAN 1085, 1081 AMSTERDAM, THE NETHERLANDS

RECEIVED NOVEMBER 27, 1996; REVISED TYPESCRIPT ACCEPTED JUNE 13, 1997

The mafic eclogites of the Lanterman Range are the first record of a well-preserved high-pressure assemblage from the Pacific end of the Transantarctic Mountains. They occur among pods and lenses (from <1 to ~30 m in size) of mafic and ultramafic metamorphic rocks that constitute a narrow zone intercalated with amphibolite-facies metasediments. This zone extends along the faulted contact between the Wilson Terrane and the Bowers Terrane, in northern Victoria Land. Most of the amphibolites and retrogressed eclogites analysed have geochemical compositions that resemble transitional to E-type mid-ocean ridge basalt (MORB) and Nd isotope data indicative of differentiation from a depleted mantle source. The age of the igneous precursors is not well determined, but Sm–Nd whole-rock data indicate a Neoproterozoic age, most probably around 700–750 Ma. For this group of metabasites a tectonic setting of an incipient ocean basin is proposed on geological and geochemical grounds. In contrast, the well-preserved eclogites are characterized by strong enrichment in more incompatible elements and pronounced negative Ta and Nb anomalies in MORB-normalized element patterns. Geochemical and Nd isotope data suggest that they are derived from a different mantle source with an enriched signature. The age of the protolith of the well-preserved eclogites, however, remains unconstrained. In the well-preserved eclogite samples the reaction textures testify to three main metamorphic stages: (1) an eclogite facies stage, (2) a medium-pressure amphibolite facies stage, and (3) a low-pressure amphibolite facies stage. The high-pressure event occurred at temperatures of up to ~850°C based on garnet and omphacite thermometry and at a minimum pressure of ~15 kbar based on the jadeitic content of omphacites. Internal Sm–Nd isochrons from two well-preserved eclogites are 500 ± 5 Ma (rutile, clinopyroxene, amphibole, whole rock and garnet) and 492 ± 3 Ma (rutile, clinopyroxene, whole rock and garnet). Rutile–whole-rock ^{238}U–^{206}Pb ages (~500 Ma) overlap the range of the Sm–Nd mineral ages. The inferred P–T *path, the microtextural features and the overlap of the Sm–Nd garnet ages with the range of the ^{238}U–^{206}Pb rutile–whole-rock ages indicate fast cooling and suggest that the time of the high-pressure event was ~500 Ma. These data place both the formation and exhumation of eclogite within a convergent plate margin setting, thus documenting the subduction–accretional nature of the early Palaeozoic Ross Orogen in northern Victoria Land.*

KEY WORDS: *Antarctica; chronology; eclogite; high-pressure metamorphism; Ross Orogen*

INTRODUCTION

Metabasites with eclogite assemblages can occur as layers and lenses of variable size within medium- to high-grade metasediments. These rocks are of particular interest as they may reveal the sites of ancient subduction zones, and therefore provide information for geodynamic reconstructions.

For kinetic and equilibrium reasons, mafic rocks tend to preserve high-pressure assemblages relative to non-mafic rocks (Koons & Thompson, 1985). This could be one of the reasons for the long-lasting controversy about the different tectonic interpretations of mafic eclogites intercalated in medium- to high-grade metasediments (see Smith, 1988), and in particular about whether the host-metasediments were present with the mafic rocks

*Corresponding author. Present address: Istituto di Geocronologia e Geochimica Isotopica–CNR, via Cardinale Maffi 36, 56100 Pisa, Italy. e-mail: iggi@iggi.pi.cnr.it

during the high-pressure event (the *in situ* eclogite model) or whether the mafic eclogites were tectonically emplaced in lower-pressure continental rocks (the foreign eclogite model).

In spite of metamorphic and tectonic reworking during the high-pressure event and subsequent retrogression, most mafic eclogites also retain the geochemical signature of the protolith, thus providing information on the tectonic framework preceding the high-pressure stage. Nevertheless, the contribution of mafic eclogites to any plate tectonic reconstruction is complete only when the timing of the eclogite facies metamorphism is constrained. Different isotope systematics have been used for this purpose, and these have been reviewed by Vidal & Hunziker (1985) and Gebauer (1990). In the last decade, many papers have demonstrated that the Sm–Nd dating technique is one of the most feasible methods, as garnet is an abundant mineral phase in eclogites. However, Sm–Nd garnet ages appear to be strongly dependent on the cooling history. Thus in slowly cooled terranes the question arises as to whether the ages represent mineral growth or subsequent cooling (Mezger *et al.*, 1992; Burton *et al.*, 1995). In contrast, in eclogites that experienced very fast tectonic burial and uplift (Schmädicke *et al.*, 1995), or in low-temperature eclogites (Thöni & Jagoutz, 1992), the lack of complete isotope homogenization during the metamorphism can yield spurious mineral ages. In some medium-temperature eclogites, the overlap of ages derived from different isotopic systems, with very different blocking temperatures, is strong evidence for fast cooling (Kalt *et al.*, 1994; Chavagnac & Jahn, 1996), thus making the closure temperature of a specific isotopic system of secondary importance (Schmädicke *et al.*, 1995).

The purpose of this paper is twofold. One is to present the first available mineralogical, geochemical, petrological and geochronological data on newly discovered well-preserved eclogites and associated amphibolites from the Lanterman Range. The Lanterman Range is at the Pacific end of the Transantarctic Mountains, and these rocks may therefore place significant constraints on the reconstruction of the thermotectonic history of the Antarctic palaeo-Pacific margin of Gondwana. The second objective is to address, in a broad perspective, the problems inherent in dating high-pressure mafic rocks.

GEOLOGICAL SETTING

Three tectonometamorphic terranes are recognized in northern Victoria Land (Fig. 1—Bradshaw & Laird, 1983): (1) the Robertson Bay Terrane, made up of a thick flysch-type sequence of Cambrian–lower Ordovician sedimentary rocks, (2) the Bowers Terrane, a Cambrian oceanic volcanic arc and related sediments (Weaver *et al.*, 1984), and (3) the Wilson Terrane, comprising low- to high-grade metamorphic rocks extensively intruded by the Granite Harbour Intrusives, a calc-alkaline association with magmatic arc affinity and of Cambro-Ordovician age [Armienti *et al.* (1990) and references therein]. During the Early Palaeozoic Ross Orogeny, both the Bowers and Robertson Bay rocks experienced low-grade metamorphism (Buggisch & Kleinschmidt, 1989), whereas a much more complex metamorphic pattern is evident in the Wilson Terrane. In the Deep Freeze Range (Fig. 1), the Wilson Terrane comprises a metasedimentary sequence (including remnants of a polymetamorphic granulite complex—Castelli *et al.*, 1991) which records a low- to high-grade metamorphism of low-pressure type (Grew *et al.*, 1984; Talarico *et al.*, 1992) with counter-clockwise P–T paths (Palmeri *et al.*, 1994). In the Lanterman, Salamander and Mountaineer ranges (Fig. 1), an intermediate-pressure belt is characterized by scattered kyanite in metapelites (Grew *et al.*, 1984; Ricci & Tessensohn, 1997*b*). At the boundary with the allochthonous Bowers Terrane, a chain of pods and lenses of mafic and/or ultramafic rocks occurs. This chain includes metabasites with eclogitic assemblages (Fig. 1—Ricci *et al.*, 1996).

The Lanterman Range and the eclogite occurrence at Husky Pass

The metamorphic sequence of the Wilson Terrane in the Lanterman Range comprises a wide variety of pelitic to quartzo-feldspathic gneisses, and minor calc-silicates, amphibolites and metamorphosed ultramafic rocks (Roland *et al.*, 1984; Kleinschmidt *et al.*, 1987). Large granitic to tonalitic plutons are apparently restricted to the western side of the range (Fig. 1) and have been assigned to the Granite Harbour Intrusives (Roland *et al.*, 1984; Kreuzer *et al.*, 1987). The metamorphic pattern of the Lanterman Range is mainly due to a major event that occurred under amphibolite facies conditions (Roland *et al.*, 1984; Kleinschmidt *et al.*, 1987). Pelitic gneisses that show incipient migmatization are confined to the northern part of the range (Mt Bernstein and Carnes Crags—Fig. 1).

The Husky Pass eclogites (Ricci *et al.*, 1996) occur as lenses of centimetric to metric thickness in the gneisses at the eastern margin of the Wilson Terrane (Fig. 1), ~2 km from the tectonic contact with the Bowers Terrane. The mafic lenses show prominent zonation with increasing degrees of retrogression of the eclogite assemblage from the centre to the edge. Ultramafic rocks (mainly serpentinites) occur locally as levels of decimetric thickness within the retrogressed eclogites. The host-rocks are mainly augen quartzo-feldspathic and pelitic gneisses and minor garnet-bearing quartzites. The occurrence of thin lenses of quartzites and quartzo-feldspathic gneisses in the internal portions of the thickest

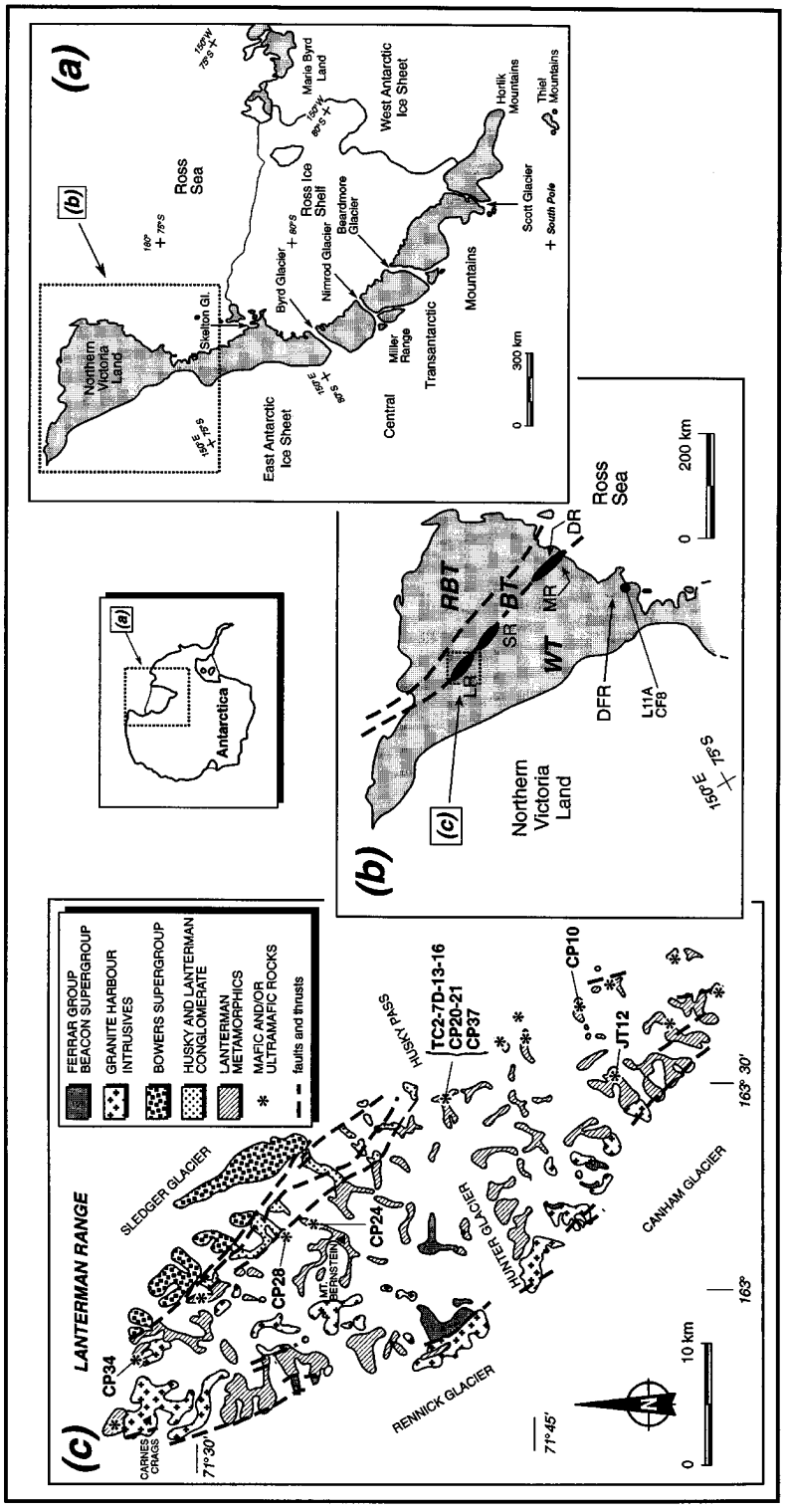

Fig. 1. (a) and (b), outcrop area (in grey) and main localities of northern Victoria Land and Central Transantarctic Mountains. RBT, Robertson Bay Terrane; BT, Bowers Terrane; WT, Wilson Terrane; LR, Lanterman Range; SR, Salamander Range; DR, Dessent Ridge; DFR, Deep Freeze Range; MR, Mountaineer Range. In black are indicated the main outcrop localities of mafic and/or ultramafic rocks. (c) Geological map of the Lanterman Range (after Roland *et al.*, 1984) and sample locations.

mafic bodies may indicate primary intrusive relationships. In addition, thin layers of serpentinites in some mafic lenses may indicate local preservation of primary igneous layering. The main foliation in both gneisses and the mafic–ultramafic lenses is deformed by isoclinal folds with axial surfaces parallel to the Ross regional trend (Capponi *et al.*, 1995).

PETROGRAPHY AND MINERAL CHEMISTRY

Eclogites

The eclogites are fine- to medium-grained rocks with grano-nematoblastic textures. Three main metamorphic stages have been recognized: (1) an eclogite facies stage, (2) a medium-pressure amphibolite facies stage, and (3) a low-pressure amphibolite facies stage. The eclogitic mineral assemblage (M1) consists of omphacite (CpxI), garnet and rutile, together with accessory quartz, apatite and zircon. Phengite and ilmenite are rarely present. Omphacite occurs as aligned elongated crystals that impart a strong compositional layering and a penetrative lineation to the eclogite. Garnets occur as small subidioblastic grains, usually 0·3 mm in size; larger grains (up to ~0·6 mm) are rare. Small inclusions of quartz, rutile, zircon and rare omphacite are enclosed in some garnets.

The first retrogressive event affecting the eclogite (medium-pressure amphibolite facies stage—M2 assemblage) induced the breakdown of CpxI to a cryptocrystalline symplectitic intergrowth of an Na-poor clinopyroxene (CpxII) and albite-rich plagioclase. During this stage, garnet is still stable, rutile is usually associated with ilmenite and there is the first appearance of amphibole. Amphibole forms either isolated crystals in apparent equilibrium with the eclogite paragenesis or poikiloblasts on garnet and omphacite.

The final stage of retrogression is characterized by extensive development of amphibole (low-pressure amphibolite facies stage—M3 assemblage). The symplectitic intergrowth of M2 assemblage was replaced by a micro- to medium-grained symplectite of amphibole + plagioclase, and garnet was rimmed by kelyphitic amphibole + epidote ± Fe oxides ± plagioclase.

Mineral chemistry was performed on three well-preserved eclogites and selected microprobe analyses are given in Table 1. Garnet compositions show the following ranges: almandine 36–54 mol %, pyrope 25–44 mol %, grossular 12–22 mol %, spessartine 1–2 mol % and andradite 0–6 mol %. In the pyrope–(almandine + spessartine)–grossular ternary diagram (Fig. 2a), garnets mainly plot within the group B eclogite field of Coleman *et al.* (1965), whereas the outermost rim compositions plot in the C field. All grains show a complementary zoning pattern for Fe and Mg, and very slight zoning for Ca, whereas Mn is nearly constant. In the ~0·3 mm sized garnets, Mg and, to a lesser degree, Ca generally decrease from the core to rim, whereas Fe shows an inverse trend (Fig. 3). The larger grains (up to ~0·6 mm) are characterized by more complex patterns (Fig. 3) that are interpreted, on the basis of compositional maps, as the result of the coalescence of small garnet nuclei (coinciding with the highest Mg contents) growing during the eclogite climax and followed by later overgrowth around the coalesced centre. CpxI are unzoned omphacites (Fig. 2b) with a jadeite component of 30–42 mol %, acmite 1–14 mol % and augite 56–57 mol %. The correlation between acmite and jadeite contents is irregular and indicates different Fe^{3+}/Fe^{2+} ratios at different points in the same grain. CpxII of the M2 assemblage is a sodic augite (Fig. 2b) with a jadeite component of 6–10 mol % and acmite 11–16 mol %. The first amphibole formed during early retrogression (M2 assemblage) is a barroisite (Leake, 1978) characterized by high Al^{IV} and very low Ti contents (Table 1). Samples that experienced extensive retrogression show CpxII + albite–oligoclase symplectite replaced by large poikiloblasts of amphibole (M3 assemblage). The latter is barroisite in the core region, and tchermakitic-hornblende towards the rim (Table 1).

Amphibolites

They are fine to medium grained with a grano-nematoblastic texture. The mineral assemblage consists of hornblende, epidote, plagioclase and quartz, with titanite, ilmenite and rare rutile as accessory minerals.

Garnet, clinopyroxene and cummingtonite are present in some samples. Garnet contains quartz and rutile inclusions and always shows resorbed edges surrounded by medium-grained amphibole ± plagioclase ± epidote kelyphite. Clinopyroxene together with plagioclase forms granoblastic sites surrounded by nematoblastic amphibole. These features, already observed in the M3 assemblage of eclogites, strongly suggest that garnet and clinopyroxene are relics of a high-pressure assemblage. Cummingtonite occurs as nematoblasts that grew together with hornblende in millimetric layers, sometimes forming poikiloblasts with inclusions of green amphibole. Rutile is generally enclosed in garnet and it and ilmenite are rimmed by titanite.

Mineral chemistry was determined on an amphibolite sample with relics of the high-pressure stage (sample CP28—Table 1). Garnet consists of 45–55 mol % of almandine, 16–27 mol % of pyrope, 18–24 mol % of grossular, 4–9 mol % of spessartine and 0–5 mol % of andradite. It shows retrograde zoning with higher Mg and lower Fe contents in the core than in the rim, whereas Ca and Mn are nearly constant. Clinopyroxene

Table 1: Representative microprobe analyses of well-preserved eclogites (TC13, TC16 and CP21), retrograded eclogite (CP28) and host-gneisses (CP37 and TC2)

Garnet											
Rock type:	Well-preserved eclogites										
Sample no.:	TC13 Grt1 rim	TC13 Grt1 p3	TC13 Grt1 p8	TC13 Grt1 p11	TC13 Grt1 core	TC13 Grt1 p22	TC13 Grt1 p24	TC13 Grt2 rim	TC13 Grt2 core	TC13 Grt2 p14	TC16 Grt1 core
SiO_2	40·22	40·05	39·73	40·19	39·51	40·50	39·97	39·58	39·87	38·77	39·83
TiO_2	—	—	—	—	—	—	—	—	—	—	—
Al_2O_3	22·45	22·30	22·39	22·63	22·33	22·78	22·25	22·27	22·51	21·85	22·49
FeO_t	19·92	19·05	21·77	18·50	21·59	19·24	22·05	23·20	19·76	23·17	20·89
MnO	0·72	0·70	0·65	0·69	0·67	0·55	0·83	0·70	0·69	0·67	0·61
MgO	10·94	11·55	9·08	10·41	9·79	11·72	9·99	8·61	9·99	8·45	10·40
CaO	6·51	6·82	7·34	8·30	6·81	6·46	6·43	6·63	7·63	6·56	6·44
Total	100·76	100·48	100·96	100·72	100·70	101·26	101·52	100·99	100·45	99·47	100·66
Si	3·00	2·99	2·99	3·00	2·98	2·99	2·99	3·00	2·99	2·98	2·99
Al	1·97	1·96	1·99	1·99	1·98	1·98	1·96	1·99	1·99	1·98	1·99
Ti	—	—	—	—	—	—	—	—	—	—	—
Fe^{3+}	0·03	0·06	0·03	0·01	0·06	0·04	0·06	0·01	0·03	0·06	0·03
Fe^{2+}	1·21	1·13	1·34	1·14	1·30	1·15	1·32	1·45	1·21	1·43	1·28
Mn	0·05	0·04	0·04	0·04	0·04	0·03	0·05	0·04	0·04	0·04	0·04
Mg	1·22	1·28	1·02	1·16	1·10	1·29	1·11	0·97	1·12	0·97	1·16
Ca	0·52	0·54	0·59	0·66	0·55	0·51	0·51	0·53	0·61	0·54	0·51
Total	8·00	8·00	8·00	8·00	8·01	8·00	8·00	8·00	7·99	8·00	8·00

Garnet									
Rock type:	Well-preserved eclogites					Retrogressed eclogites			
Sample no.:	TC16 Grt1 rim	TC16 Grt2 core	TC16 Grt2 rim	CP21 Grt rim	CP21 Grt core	CP28 Grt1 rim	CP28 Grt1 core	CP28 Grt2 rim	CP28 Grt2 core
SiO_2	39·55	39·89	39·55	39·34	39·46	38·39	38·88	38·14	39·44
TiO_2	—	—	—	—	—	—	0·24	—	—
Al_2O_3	22·39	22·03	21·95	22·87	22·66	21·87	21·73	21·97	22·00
FeO_t	22·79	20·26	22·34	22·76	22·17	24·32	22·33	26·03	22·08
MnO	0·51	0·58	0·64	0·64	0·74	2·38	2·28	1·78	2·05
MgO	9·07	10·87	9·49	7·87	9·29	5·31	6·87	5·46	8·08
CaO	6·33	6·62	6·40	7·89	6·95	8·03	8·39	7·51	7·07
Total	100·64	100·59	100·37	101·37	101·27	100·30	100·72	100·96	100·72
Si	2·99	2·99	3·00	2·97	2·96	2·98	2·98	2·95	3·00
Al	2·00	1·95	1·96	2·03	2·00	2·00	1·96	2·00	1·97
Ti	—	—	—	—	—	—	0·01	—	—
Fe^{3+}	0·02	0·07	0·04	0·00	0·03	0·03	0·06	0·10	0·03
Fe^{2+}	1·42	1·20	1·37	1·44	1·35	1·54	1·37	1·58	1·38
Mn	0·03	0·03	0·04	0·04	0·05	0·16	0·15	0·12	0·13
Mg	1·02	1·22	1·07	0·88	1·04	0·61	0·78	0·63	0·92
Ca	0·51	0·53	0·52	0·64	0·56	0·67	0·69	0·62	0·58
Total	8·00	8·00	8·00	8·00	7·99	7·99	8·00	8·00	8·00

Table 1: continued

Garnet						*Clinopyroxene*			
Rock type:	Host-gneisses					Rock type:	Well-preserved eclogites		
Sample no.:	CP37 Grt1 rim	CP37 Grt1 core	CP37 Grt1 p22	TC2 Grt rim	TC2 Grt core	Sample no.:	TC13 Cpx1 rim	TC13 Cpx2 core	TC13 Cpx3
SiO_2	37·34	37·84	37·06	38·44	38·45	SiO_2	53·74	54·78	55·0
TiO_2	—	—	—	—	—	TiO_2	—	—	—
Al_2O_3	21·25	21·33	21·20	22·30	22·24	Al_2O_3	10·31	9·17	10·20
FeO_t	25·32	23·46	24·27	23·80	23·72	Cr_2O_3	—	—	—
MnO	12·85	13·82	12·58	0·27	0·41	FeO_t	6·44	6·56	5·52
MgO	3·15	3·12	3·40	3·74	3·74	MnO	—	—	—
CaO	0·91	1·47	1·16	12·20	12·00	MgO	8·60	8·53	8·84
Total	100·82	101·05	99·67	100·75	100·56	CaO	14·07	14·29	14·33
						Na_2O	5·73	5·89	5·91
Si	2·98	3·00	2·99	2·97	2·98	K_2O	—	—	—
Al	2·00	2·00	2·01	2·03	2·03	Total	98·89	99·22	99·85
Ti	—	—	—	—	—				
Fe^{3+}	0·03	0·00	0·01	0·02	0·01	Si	1·95	1·99	1·97
Fe^{2+}	1·66	1·56	1·62	1·52	1·53	Al^{IV}	0·05	0·01	0·03
Mn	0·87	0·93	0·86	0·02	0·03	Al^{VI}	0·39	0·38	0·40
Mg	0·37	0·37	0·41	0·43	0·42	Ti	—	—	—
Ca	0·08	0·12	0·10	1·01	1·00	Cr	—	—	—
Total	7·99	7·98	8·00	8·00	8·00	Fe^{3+}	0·06	0·04	0·03
						Fe^{2+}	0·13	0·16	0·14
						Mn	—	—	—
						Mg	0·46	0·46	0·47
						Ca	0·55	0·55	0·55
						Na	0·40	0·41	0·41
						K	—	—	—
						Total	4·00	4·00	4·00

is a salite with low acmite and jadeite components (~1 mol %). Plagioclase ranges in composition from anorthite 48 mol % in the kelyphite to anorthite 24 mol % where it is associated with clinopyroxene. Amphibole is unzoned and ranges in composition from tschermakite hornblende to Mg-hornblende (Leake, 1978) (Table 1).

Host-rocks

The rocks hosting the metabasites are medium-grained gneisses with minor quartzites and are characterized by a grano-lepidoblastic texture consisting of quartz, plagioclase, biotite, muscovite, ±K-feldspar, ±epidote, ±amphibole, ±garnet, ±fibrolitic sillimanite. Accessory minerals include zircon, apatite, ilmenite, allanite and rutile. In the pelitic gneisses, garnet is euhedral, up to 3 mm in size, and generally shows inclusion-rich cores and inclusion-free rims. The inclusions consist of quartz, plagioclase, biotite, muscovite and ilmenite, which also constitute the matrix of the rocks. In the quartzo-feldspathic rocks and quartzites, garnet (up to 0·2 mm in size) is sub-euhedral to anhedral and is surrounded by fine-grained symplectite consisting of plagioclase + biotite + quartz. Similar symplectites are also found around relict phengite. Sillimanite shows wisp-like needles associated with biotite and quartz, and sometimes resembles 'disthene-sillimanite' (Marchand, 1974). Clear relict kyanite, however, has only been found in plagioclase (B. Ghiribelli, personal communication, 1996).

Table 1: continued

Clinopyroxene								*Amphibole*		
Rock type:	Well-preserved eclogites						Retrogressed eclogite	Well-preserved eclogites		
Sample no.:	TC13 Cpx symplectite	TC16 Cpx1 rim	TC16 Cpx1 core	TC16 Cpx2 rim	TC16 Cpx2 core	CP21 Cpx core	CP28 Cpx1 matrix	TC13 Cam core	TC13 Cam rim	TC16 Cam rim
SiO_2	50·10	54·60	54·65	54·12	53·88	54·37	51·84	45·85	45·43	45·72
TiO_2	0·24	—	—	—	—	0·20	—	0·37	0·33	0·20
Al_2O_3	7·23	8·92	9·20	8·87	9·02	8·85	1·15	13·25	15·47	15·33
Cr_2O_3	—	—	—	—	—	—	—	—	0·09	—
FeO_t	10·23	7·09	7·82	7·04	7·45	7·77	11·82	11·19	11·75	11·67
MnO	—	—	—	—	—	—	—	—	—	—
MgO	11·33	8·86	8·38	9·14	8·42	8·71	11·39	12·95	11·78	11·46
CaO	17·83	13·96	13·95	13·90	13·35	14·91	22·99	8·52	8·72	8·62
Na_2O	2·35	5·84	5·85	5·66	6·29	5·57	0·36	3·35	3·22	3·38
K_2O	—	—	—	—	—	—	—	0·36	0·21	0·20
Total	99·31	99·27	99·85	98·73	98·41	100·38	99·85	95·84	97·00	96·58
Si	1·87	1·97	1·97	1·97	1·96	1·96	1·97	6·66	6·46	6·55
Al^{IV}	0·13	0·03	0·03	0·03	0·04	0·04	0·03	1·34	1·54	1·45
Al^{VI}	0·19	0·35	0·36	0·35	0·35	0·34	0·02	0·88	1·06	1·14
Ti	0·01	—	—	—	—	0·01	—	0·04	0·04	0·02
Cr	—	—	—	—	—	—	—	—	0·01	—
Fe^{3+}	0·10	0·07	0·07	0·08	0·13	0·07	0·01	0·79	0·81	0·65
Fe^{2+}	0·19	0·14	0·16	0·13	0·10	0·14	0·36	0·54	0·59	0·74
Mn	—	—	—	—	—	—	—	—	—	—
Mg	0·63	0·48	0·45	0·50	0·46	0·47	0·64	2·74	2·50	2·45
Ca	0·71	0·54	0·54	0·54	0·52	0·58	0·94	1·30	1·33	1·32
Na	0·17	0·41	0·41	0·40	0·44	0·39	0·03	0·92	0·89	0·94
K	—	—	—	—	—	—	—	0·07	0·04	0·04
Total	4·00	3·99	3·99	4·00	4·00	4·00	4·00	15·29	15·26	15·30

Microprobe analyses (Table 1) were performed on garnet, biotite, muscovite and plagioclase from a pelitic gneiss (sample CP37) and a quartzo-feldspathic gneiss (sample TC2). In the pelitic gneiss, garnet is spessartine-rich almandine with slight zoning characterized by a higher spessartine and grossular component and lower almandine component in the core with respect to the rim (Table 1). In the quartzo-feldspathic gneiss, garnet is homogeneous spessartine-poor almandine with a high grossular component (Table 1). Biotite is compositionally homogeneous with $X_{Mg} = 0{\cdot}50$ in pelitic gneiss and 0·57 in the quartzo-feldspathic gneiss. Muscovite is characterized by low phengite and paragonite contents [Si up to 3·2–3·3 atoms on 11 oxygens and Na/(Na + K) up to 0·08]. Plagioclase is homogeneous and ranges in composition from anorthite 13 mol % in the pelitic gneiss to anorthite 30 mol % in the quartzo-feldspathic sample.

THERMOBAROMETRY

Mafic rocks

Eclogite facies stage

Temperatures were estimated using different geothermometer calibrations based on Fe–Mg exchange reactions between garnet and clinopyroxene (see Table 2).

Table 1: continued

Amphibole						*Biotite*				
Rock type:	Well-preserved eclogites		Retrogressed eclogites			Host-gneisses				
Sample no.:	TC16 Cam core	CP21 Cam core	CP28 Cam3 matrix	CP28 Cam1 kelyphite	CP28 Cam2 kelyphite	CP37 Bt1	CP37 Bt3 matrix	CP37 Bt4 matrix	TC2 Bt1 matrix	TC2 Bt2 matrix
SiO_2	46·48	46·37	42·42	42·85	42·40	36·11	35·97	36·30	37·39	37·56
TiO_2	0·37	0·40	0·72	1·36	1·13	2·58	2·66	2·93	2·29	2·37
Al_2O_3	13·95	12·59	14·29	13·16	13·66	19·87	19·68	19·60	17·71	17·69
Cr_2O_3	—	—	—	0·13	0·05	—	—	—	—	—
FeO_t	10·85	14·88	17·12	17·28	16·74	17·22	17·93	17·28	16·76	16·56
MnO	—	0·07	0·30	0·30	0·19	0·39	0·46	0·46	—	—
MgO	13·61	11·83	9·12	9·27	9·40	10·44	10·03	9·82	12·78	12·88
CaO	8·35	8·51	11·70	11·60	11·83	—	—	—	—	—
Na_2O	3·96	3·39	1·39	1·45	1·33	0·13	0·13	0·11	0·07	—
K_2O	0·42	0·10	0·95	0·87	0·87	10·07	10·00	9·97	9·27	9·16
Total	97·99	98·14	98·01	98·27	97·61	96·81	96·98	96·56	96·24	96·22
Si	6·53	6·67	6·27	6·33	6·29	5·36	5·36	5·41	5·54	5·56
Al^{IV}	1·47	1·33	1·73	1·67	1·71	2·64	2·64	2·59	2·46	2·44
Al^{VI}	0·84	0·81	0·76	0·62	0·68	0·84	0·82	0·85	0·63	0·64
Ti	0·04	0·04	0·08	0·15	0·13	0·29	0·30	0·33	0·25	0·26
Cr	—	—	—	0·01	0·01	—	—	—	—	—
Fe^{3+}	0·89	0·84	0·53	0·48	0·45	—	—	—	—	—
Fe^{2+}	0·39	0·76	1·58	1·65	1·63	2·14	2·23	2·15	2·08	2·05
Mn	—	0·01	0·04	0·04	0·02	0·05	0·06	0·06	—	—
Mg	2·85	2·54	2·01	2·04	2·08	2·31	2·23	2·18	2·82	2·84
Ca	1·26	1·31	1·85	1·84	1·88	—	—	—	—	—
Na	1·08	0·95	0·40	0·41	0·38	0·04	0·04	0·03	0·02	—
K	0·08	0·02	0·18	0·16	0·16	1·91	1·90	1·89	1·74	1·73
Total	15·41	15·28	15·43	15·41	15·43	15·58	15·58	15·49	15·54	15·52

The thermometric data of the eclogitic stage were calculated using garnet and omphacite in well-preserved microtextural sites, where the absence of retrograde phases suggested that the eclogite paragenesis recorded the climax conditions. Moreover, the fact that the K_D determined between garnet and omphacite varied in a narrow range in a single sample (Table 2), is indicative of chemical equilibrium in the sites where thermobarometry was evaluated. For garnet, core compositions of smaller crystals or the inner rim of larger garnets were used; for omphacites low acmite content omphacites were utilized.

Temperatures estimated using the Ai Yang (1994) calibration (Table 2) were in the range 720–850°C for smaller garnets and around 840°C for larger garnets. An important observation was that the temperatures obtained in the smallest garnets overlapped those in the largest ones. Minimum pressure estimations on the basis of the jadeitic content of omphacite in the presence of quartz (Holland, 1983) were ~15 kbar at 800°C.

Medium-pressure amphibolite facies stage

Retrograde zoning in garnets suggests that rim compositions of garnet and omphacite in mutual contact, even in sites where eclogite assemblage is well preserved, can be used to constrain early retrograde conditions. Temperatures in the range 630–750°C were obtained in both small and large garnets [calibration of Ai Yang (1992), Table 2].

Pressures were evaluated using the jadeitic content of clinopyroxene in symplectite (Holland, 1983) and by

Table 1: continued

Muscovite					*Plagioclase*					
Rock type:	Host-gneisses				Rock type:	Host-gneisses				
Sample no.:	CP37 Ms1	CP37 Ms2 matrix	TC2 Ms1 matrix	TC2 Ms2 matrix	Sample no.:	CP37 Pl1 rim	CP37 Pl1 core	CP37 Pl2 core	TC2 Pl rim	TC2 Pl core
SiO_2	45·89	46·21	50·53	49·35	SiO_2	65·27	65·55	65·04	59·68	59·25
TiO_2	0·75	0·81	0·83	0·68	Al_2O_3	22·99	22·49	22·57	25·15	25·70
Al_2O_3	36·13	36·60	27·98	29·29	CaO	2·57	2·25	2·64	6·22	7·20
Cr_2O_3	—	—	—	—	Na_2O	9·55	9·76	9·35	8·77	7·97
FeOt	1·86	1·74	3·65	3·45	K_2O	0·07	0·22	0·30	0·26	—
MnO	—	—	—	—	Total	100·45	100·27	99·90	100·13	100·16
MgO	0·96	0·86	2·92	2·33						
CaO	—	—	—	—	Si	2·85	2·87	2·86	2·66	2·64
Na_2O	0·33	0·55	—	—	Al	1·18	1·16	1·17	1·32	1·35
K_2O	9·53	9·79	10·49	10·73	Ca	0·12	0·10	0·12	0·30	0·34
Total	95·46	96·59	96·40	95·83	Na	0·81	0·83	0·79	0·76	0·69
					K	0·01	0·01	0·02	0·01	—
Si	6·07	6·05	6·70	6·60	Total	4·97	4·97	4·96	5·05	5·02
Al^{IV}	2·36	2·35	1·30	1·40						
Al^{VI}	3·27	3·30	3·08	3·21						
Ti	0·07	0·08	0·08	0·07						
Cr	—	—	—	—						
Fe^{3+}	—	—	—	—						
Fe^{2+}	0·21	0·19	0·40	0·38						
Mn	—	—	—	—						
Mg	0·19	0·17	0·58	0·46						
Ca	—	—	—	—						
Na	0·08	0·14	—	—						
K	1·61	1·64	1·77	1·83						
Total	13·43	13·52	13·91	13·95						

Ferrous and ferric iron contents for garnet and clinopyroxene were calculated according to Ryburn *et al.* (1976). Ferrous and ferric iron contents for amphibole were determined by charge balance. Structural formulae were calculated on the basis of 12 oxygens for garnet, 6 for clinopyroxene, 13 for epidote, 22 for micas, 8 for plagioclase and 23 oxygens and 13 cations excluding Ca + Na + K for amphibole.

the plagioclase–clinopyroxene–garnet–quartz barometer (Newton & Perkins, 1982) using symplectite phases and garnet rim. However, the barometer could only be used in a few microstructural sites, which yielded pressures of 10 kbar at 700°C (Table 3). Pressures evaluated through the jadeitic content of CpxII at 700°C were 5–6 kbar, but the low jadeitic content of CpxII yields less precise and semiquantitative pressure estimations (Godard, 1988) compared with the eclogitic stage pressure.

Low-pressure amphibolite facies stage

Extensive development of amphibole in the mafic rocks allows temperatures and pressures to be estimated by the experimental calibration of Plyusnina (1982) based on Ca and Al concentrations of coexisting plagioclase and amphibole. These results were compared with those obtained by the qualitative methods of Spear (1980) and Brown (1977). In the retrogressed eclogite CP28, temperature was also estimated through the Fe–Mg exchange between garnet rims and the kelyphitic amphibole (Graham & Powell, 1984). The Plyusnina (1982) calibration yielded a wide range of values for temperature and pressure. Temperature ranged from 525 to 625°C and pressure from 4 to 8 kbar. A similar temperature range (500–650°C) was obtained using the method of Spear (1980). Higher temperatures (670–730°C) were estimated through the Fe–Mg exchange between garnet

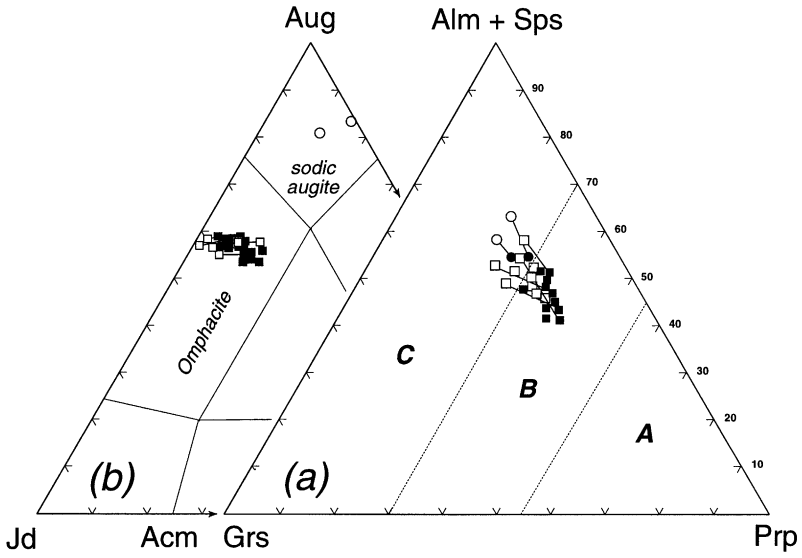

Fig. 2. Garnet (a) and pyroxene (b) compositions plotted after Coleman *et al.* (1965) and Essene & Fyfe (1967), respectively. Pyroxene end-members are augite (Aug), jadeite (Jd) and acmite (Acm). Garnet end-members are almandine + spessartine (Alm + Sps), grossular (Grs) and pyrope (Prp). A, B and C fields represent the compositional variations of garnets in eclogites associated with kimberlites and peridotites (A), with gneisses (B) and with blueschists (C). Open symbols represent rim compositions. In the garnet diagram (a), square symbols refer to well-preserved eclogites and circles to retrogressed eclogite. Open circles in the pyroxene diagram (b) represent sodic augite in symplectite.

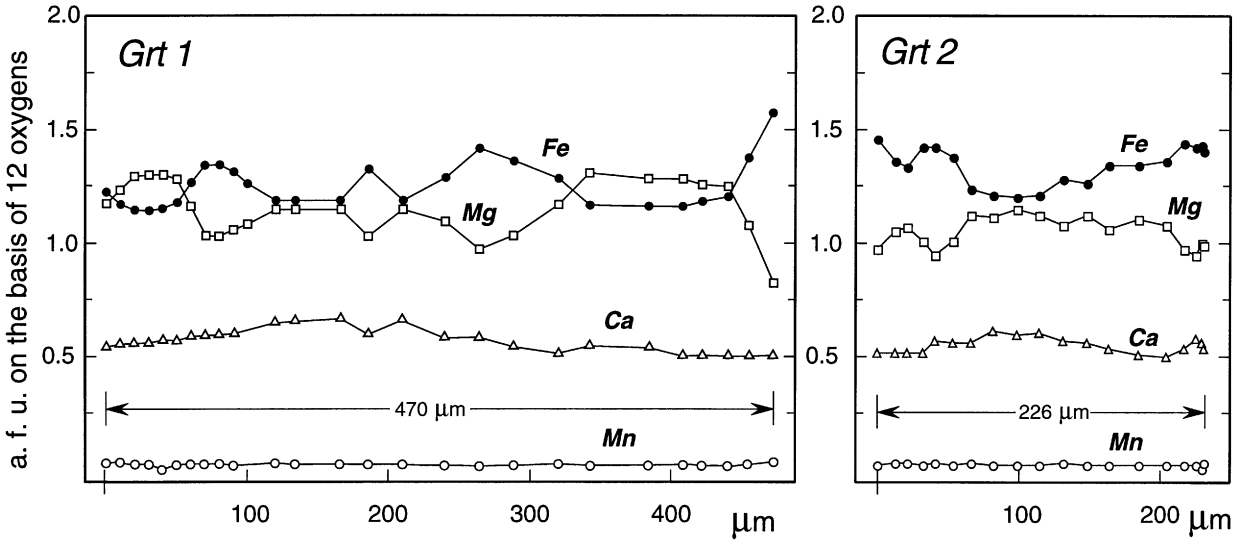

Fig. 3. Atomic profiles across two garnets of different size of a well-preserved eclogite (sample TC13).

and amphibole in kelyphites (Table 3). A qualitative pressure evaluation, based on Al^{IV} and Na (M4) of amphibole (Brown, 1977) indicated higher pressures of formation (7 kbar) for early barroisitic amphibole (medium amphibolite stage) than for late tschermakitic and Mg-hornblende (3 kbar). The latter empirical estimate agrees with the microstructural and chemical data on barroisites and tschermakitic hornblende, as the increase in Al^{IV} and Ca in the M4 site indicates that tschermakitic hornblende developed at relatively constant temperature and lower pressure than barroisites (Ungaretti *et al.*, 1981; and personal communication, 1996).

Host-rocks

Temperatures were evaluated using the thermometer based on the Fe–Mg exchange between garnet and biotite

*Table 2: Equilibrium temperatures (°C) for well-preserved eclogites based on the Fe–Mg distribution in coexisting garnet–omphacite pairs (*P = *16 kbar), using the calibrations of Ellis & Green (1979; EG); Krogh (1988; K); Ai Yang (1994; AI); Powell (1985; P)*

Sample	X_{Mg} Grt	X_{Mg} Cpx	X_{Ca} Grt	*mg*-no. Grt	ln K_D	EG (°C)	K (°C)	AI (°C)	P (°C)
TC13									
Grt1p24–$Cpx1_{rim}$	0·46	0·78	0·14	45·68	1·44	817	739	702	796
Grt1p22–$Cpx1_{rim}$	0·53	0·78	0·15	52·87	1·15	930	874	822	914
Grt1p11–$Cpx1_{rim}$	0·50	0·78	0·22	50·43	1·25	956	940	867	943
$Grt2_{rim}$–Cpx3	0·40	0·77	0·17	40·08	1·61	790	730	689	770
$Grt2_{core}$–Cpx3	0·48	0·77	0·19	48·07	1·29	915	881	821	900
TC16									
$Grt1_{rim}$–$Cpx1_{rim}$	0·42	0·77	0·16	41·80	1·56	795	729	690	775
$Grt1_{core}$–$Cpx1_{core}$	0·48	0·74	0·16	47·54	1·13	941	889	852	926
$Grt2_{rim}$–$Cpx2_{rim}$	0·44	0·79	0·15	43·85	1·13	779	706	664	757
$Grt2_{core}$–Cpx2	0·50	0·79	0·14	50·41	1·33	854	782	734	835
CP21									
Grt_{rim}–Cpx_{rim}	0·38	0·77	0·21	37·93	1·70	799	758	707	780
Grt_{core}–Cpx_{core}	0·44	0·77	0·17	43·51	1·47	834	779	733	815

Mineral analyses are from Table 1.

(Ferry & Spear, 1978; Indares & Martignole, 1985; Perchuck *et al.*, 1985). Pressures were calculated using the garnet–sillimanite–plagioclase–quartz barometer (Newton & Haselton, 1981; Perchuck *et al.*, 1985), the phengite content of muscovite (Massonne & Schreyer, 1987), and the garnet–muscovite–biotite–plagioclase thermo-barometer (Ghent & Stout, 1981). The highest temperatures (625–730°C, Table 3) were obtained using core and/or inner rim compositions of the mineralogical phases of the matrix whereas the lowest temperatures (585–630°C, Table 3) were obtained using rim compositions of phases in mutual contact. The highest pressure (12 kbar, Table 3) was obtained with the garnet–sillimanite–plagioclase–quartz barometer in sample CP37. In the same sample, the Ghent & Stout (1981) barometer gave lower pressures (~7 kbar) indicating that muscovite recorded lower-pressure conditions. In quartzo-feldspathic rock (sample TC2), a pressure of 10 kbar was obtained for core and rim compositions of the mineral phases, using the barometers of Ghent & Stout (1981) and Massonne & Schreyer (1987).

GEOCHEMICAL AND ISOTOPE DATA

Major and trace elements

Whole-rock major and trace element data for nine selected metabasites (two well-preserved eclogites, two retrogressed eclogites and five amphibolites) are reported in Table 4. They show normative parameters ranging from Ne-normative to Hy-normative basalts and, except for retrogressed eclogite CP20, are characterized by TiO_2 enrichment correlated with Fe enrichment. Sample CP20 has anomalous compositions for most of the elements considered (e.g. low TiO_2 and low Zr/Y ratio) and could have been involved in chemical modification phenomena during the metamorphic events. The other samples do not display collinear distribution for most of the immobile elements, suggesting that they are not cogenetic.

When plotted on different discrimination diagrams (Pearce & Cann, 1973; Pearce & Norry, 1979; Wood *et al.*, 1979; Pearce, 1982; Mullen, 1983; Meschede, 1986), most of the samples analysed fell in the mid-ocean ridge basalt field (both N- and E-type MORB). It is noteworthy that the two well-preserved eclogites (TC13 and TC16) plotted in the field representative of the volcanic-arc basalts or mafic rocks modified by continental crust, in the Th–Hf–Ta triangular diagram (Wood *et al.*, 1979). However, the distribution of the data points in the Ti/Cr vs Ni (Beccaluva *et al.*, 1979), Ti vs Cr (Pearce, 1975) and Ti vs V (Shervais, 1982) discrimination diagrams did not coroborate a volcanic-arc affinity. Most of the samples analysed had La/Ta ratios (Fig. 4) between 18 and 11 (~18·5 and ~10 are typical for N-MORB and E-MORB, respectively; Saunders, 1984). As for Th–Hf–Ta relationships, the two well-preserved eclogites strongly deviated from this range, with La/Ta ratios up to 47.

Table 3: Geothermobarometric data of the host-gneisses and of the retrogressed stages of eclogites

Sample	*X*pyr	*X*grs	*X*phl	*X*an	Si^{4+}	*X*K	XAl^{VI}	*X*Mg	*X*Mg	*T* (°C)	*T* (°C)	*T* (°C)	*T* (°C)	*T* (°C)	*P* (kbar)	*P* (kbar)	*P* (kbar)	*P* kbar)	*P* (kbar)
	Grt	Grt	Bt	Pl	Ms	Ms	Ms	Hbl	Cpx	P	FS	IM	GS	GP	NP	P	NH	GS	MS
Host-gneisses																			
CP37																			
Grt_{core}–Bt3	0·12	0·04	0·40	—	—	—	—	—	—	622	693	790	—	—	—	—	—	—	—
Grt_{core}–Bt3–$Pl1_{core}$–Ms2	0·12	0·04	0·40	0·11	3·02	0·92	0·88	—	—	—	—	—	690	—	—	—	—	6·9	—
Grt_{core}–Bt4	0·12	0·04	0·40	—	—	—	—	—	—	619	687	771	—	—	—	—	—	—	—
Grt_{core}–Bt4–$Pl2_{core}$–Ms2	0·12	0·04	0·40	0·13	3·02	0·92	0·88	—	—	—	—	—	682	—	—	—	—	6·3	—
Grtp22–Bt4	0·14	0·03	0·40	—	—	—	—	—	—	627	716	771	—	—	—	—	—	—	—
Grtp22–Bt4–$Pl1_{core}$–Ms2	0·14	0·03	0·40	0·11	3·02	0·92	0·88	—	—	—	—	—	710	—	—	—	—	6·7	—
$Grt1_{rim}$–Bt1	0·12	0·03	0·41	—	—	—	—	—	—	584	636	708	—	—	—	—	—	—	—
$Grt1_{rim}$–Bt1–$Pl1_{rim}$–Ms1	0·12	0·03	0·41	0·13	3·03	0·95	0·87	—	—	—	—	—	628	—	—	—	—	4·9	—
Grt_{core}–$Pl1_{core}$	0·12	0·03	—	0·11	—	—	—	—	—	—	—	—	—	—	—	10	9·5	—	—
Grt_{core}–$Pl2_{core}$	0·12	0·04	—	0·13	—	—	—	—	—	—	—	—	—	—	—	9	8·4	—	—
Grtp22–$Pl1_{core}$	0·14	0·03	—	0·11	—	—	—	—	—	—	—	—	—	—	—	12	12	—	—
Grt_{rim}–$Pl1_{rim}$	0·12	0·03	—	0·13	—	—	—	—	—	—	—	—	—	—	—	9·9	9·9	—	—
TC2																			
Grt_{core}–Bt1	0·14	0·34	0·49	—	—	—	—	—	—	730	631	745	—	—	—	—	—	—	—
Grt_{core}–Bt1–Pl_{core}–Ms1	0·14	0·34	0·49	0·33	3·3	1·00	0·74	—	—	—	—	—	638	—	—	—	—	9·4	10
Grt_{rim}–Bt2	0·14	0·34	0·49	—		—	—	—	—	—	—	—	—	—	—	—	—	—	—
Grt_{rim}–Bt2–Pl_{rim}–Ms2	0·14	0·34	0·49	0·28	3·3	1·00	0·78	—	—	733	634	721	630	—	—	—	—	10	10
Retrogressed eclogite																			
CP28																			
$Grt1_{rim}$–Cam1	0·20	0·21	—	—	—	—	—	0·55	—	—	—	—	—	730	—	—	—	—	—
$Grt2_{rim}$–Cam2	0·21	0·16	—	—	—	—	—	0·56	—	—	—	—	—	674	—	—	—	—	—
Well–preserved eclogite																			
TC13																			
$Grt2_{rim}$–Cpx–Pl	0·32	0·17	—	0·22	—	—	—	—	0·63	—	—	—	—	—	10	—	—	—	—
$Grt2_{rim}$–Cpx–Pl	0·33	0·16	—	0·22	—	—	—	—	0·63	—	—	—	—	—	10	—	—	—	—

Garnet–biotite thermometer: P, Perchuck *et al.* (1985); FS, Ferry & Spear (1978); IM, Indares & Martignole (1985). Garnet–plagioclase–muscovite–biotite thermobarometer: GS, Ghent & Stout (1981). Garnet–plagioclase–sillimanite–quartz barometer: NH, Newton & Haselton (1981); P, Perchuk *et al.* (1985). Phengite barometry: MS, Massonne & Schreyer (1987). Garnet–plagioclase–clinopyroxene–quartz barometer on symplectites: NP, Newton & Perkins (1982). Garnet–hornblende thermometer: GP, Graham & Powell (1984). Analyses used in the calculation are reported in Table 1.

Table 4: Major and trace element results

Sample:	TC7D	TC13	TC16	CP10	CP20	CP24	CP28	CP34	JT12
	A	WPE	WPE	A	RE	A	RE	A	A
Major elements (wt %)									
SiO_2	44·40	46·85	46·13	45·68	51·54	47·82	48·80	44·71	48·59
TiO_2	1·73	1·43	1·72	2·03	0·29	1·14	1·61	1·25	0·75
Al_2O_3	14·67	14·22	14·45	13·88	14·47	14·73	14·04	12·77	14·99
Fe_2O_{3t}	13·70	12·96	14·46	16·45	11·02	11·07	11·92	10·55	10·20
MnO	0·26	0·20	0·19	0·30	0·19	0·16	0·18	0·16	0·16
MgO	8·84	8·49	8·45	6·68	7·84	7·67	6·55	8·06	8·56
CaO	9·48	11·82	10·89	10·73	9·57	11·11	11·25	17·40	12·59
Na_2O	2·73	3·51	3·28	2·69	3·13	2·88	2·80	1·66	1·90
K_2O	1·23	0·044	0·18	0·21	0·59	1·02	0·76	0·43	0·74
P_2O_5	0·32	0·36	0·26	0·25	0·09	0·16	0·21	0·18	0·12
LOI	1·64	0·16	0·22	0·70	0·75	2·08	1·31	2·13	0·60
Sum	99·00	100·04	100·23	99·60	99·48	99·84	99·43	99·30	99·20
mg-no.	54·2	61·0	56·4	52·7	59·8	63·3	61·8	73·9	67·9
Trace elements (p.p.m.)									
Ni	159	162	54	95	94	72	55	63	137
Co	50	51	51	36	43	41	38	34	42
Cr	442	468	118	161	303	245	149	152	322
V	233	271	270	430	238	285	259	237	270
Sc	24	32	35	32	31	27	26	27	29
Cu	22	18	17	18	9·6	37	7·6	57	47
Zn	90	108	114	95	71	78	84	67	57
Ga	20	14	15	20	13	17	18	16	15
Pb	4·8	4·2	1·5	2·3	6·1	1·7	13	4·2	2·9
Sr	66	49	32	103	36	84	136	155	164
Rb	41	2·0	9·1	1·9	24	47	25	11	23
Ba	305	3·2	15	6·9	65	42	60	45	109
Zr	118	93	107	127	14	70	114	82	43
Hf	3·0	2·4	2·9	3·4	0·4	1·9	2·9	2·1	1·2
Nb	15	5·0	6·0	2·0	1·2	2·7	9·1	5·3	2·1
Ta	0·97	0·38	0·48	0·16	0·12	0·20	0·70	0·38	0·17
Th	2·6	6·2	3·4	0·18	0·38	0·36	0·98	0·42	0·33
U	0·12	0·64	0·38	0·11	0·29	0·23	0·81	0·27	0·23
Y	28	26	32	54	15	29	32	29	16
La	12	18	12	2·9	1·3	2·9	9·4	5·1	2·5
Ce	34	41	27	9·3	2·9	8·1	22	13	6·7
Pr	4·2	5·4	3·4	1·8	0·35	1·3	3·1	2·0	1·0
Nd	19	22	15	11	1·8	7·4	15	9·9	5·1
Sm	4·3	5·3	3·4	4·8	0·65	2·7	4·9	3·5	1·7
Eu	1·1	1·1	0·68	1·9	0·27	1·0	1·5	1·16	0·72
Gd	3·6	3·4	2·4	6·2	1·0	3·3	4·63	3·6	2·0
Tb	0·64	0·49	0·49	1·4	0·26	0·68	0·91	0·76	0·4
Dy	4·6	3·6	4·2	8·8	2·1	4·4	5·5	4·8	2·5
Ho	1·1	1·0	1·3	2·0	0·53	1·1	1·2	1·1	0·64
Er	2·6	3·0	3·4	5·2	1·5	2·7	3·0	2·7	1·6
Tm	0·40	0·49	0·56	0·83	0·28	0·44	0·45	0·43	0·23
Yb	2·6	3·3	3·5	5·7	2·2	2·8	3·1	2·7	1·7
Lu	0·37	0·52	0·57	0·89	0·34	0·47	0·51	0·48	0·25
$(La/Sm)_N$	1·84	2·19	2·22	0·39	1·25	0·69	1·24	0·95	0·95
$(La/Yb)_N$	3·39	3·93	2·35	0·36	0·42	0·74	2·20	1·35	1·07
Eu/Eu*	0·87	0·77	0·72	1·06	1·03	1·04	0·96	1·00	1·19

WPE, well-preserved eclogites; RE, retrogressed eclogites; A, amphibolites; *mg*-no., molar $Mg/(Mg+Fe^{2+})$ assuming $Fe_2O_3/FeO=0{\cdot}15$.

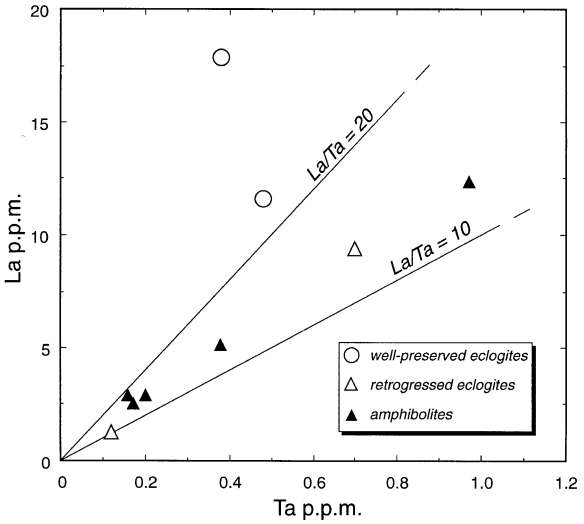

Fig. 4. La vs Ta diagram for well-preserved eclogites, retrogressed eclogites and amphibolites from Lanterman Range.

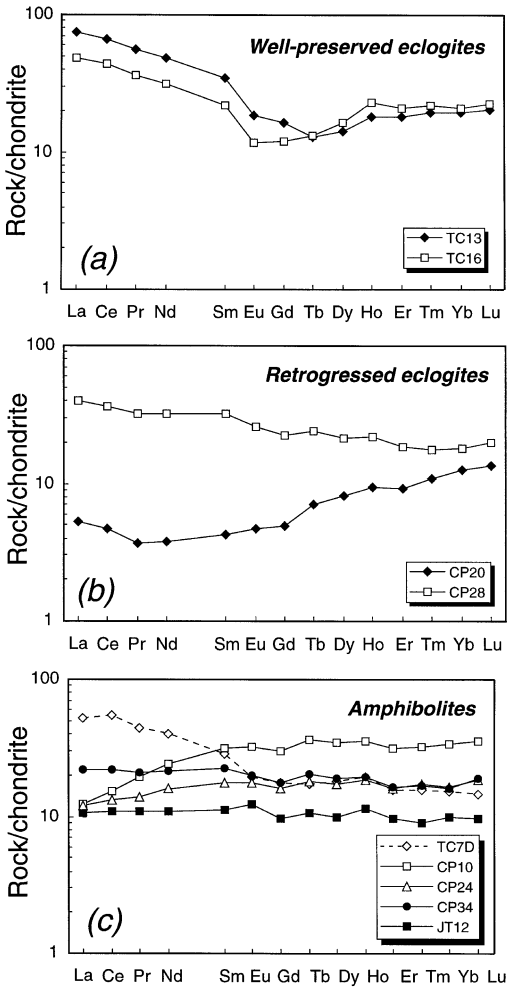

Fig. 5. REE chondritic patterns for well-preserved eclogites (a), retrogressed eclogites (b) and amphibolites (c). Chondritic values are from Sun & McDonough (1989).

The REE distribution patterns for retrogressed eclogites and amphibolites (Fig. 5b and c) ranged from light rare earth element (LREE) depleted (i.e. sample CP10) with $(La/Sm)_N = 0{\cdot}39$ and unfractionated heavy REE (HREE), essentially unfractionated patterns (e.g. sample CP34) at abundances of ~20 × chondrite, to LREE enriched (i.e. sample TC7D) with $(La/Sm)_N = 1{\cdot}84$ and abundances of ~50 × chondrite for La. Sample CP20 had low REE abundances (La 5·5 × chondritic value) and a pattern similar to some anomalous profiles as described for eclogite rocks elsewhere (Griffin & Brueckner, 1985; Paquette *et al.*, 1989; Bernard-Griffiths *et al.*, 1991). Most of the samples lacked pronounced Eu anomalies, except for sample TC7D, which showed a slight negative anomaly ($Eu/Eu^* = 0{\cdot}87$), and sample JT12, characterized by a positive Eu anomaly ($Eu/Eu^* = 1{\cdot}19$). The latter feature may be attributed to minor cumulate plagioclase. The two well-preserved eclogites (Fig. 5a) showed strong LREE enrichment [$(La/Sm)_N > 2$] with abundances of ~50–75 × chondrite for La and negative Eu anomaly [$(Eu/Eu^*) = 0{\cdot}77$–$0{\cdot}72$].

In Fig. 6a–c expanded REE patterns and a range of incompatible elements are used to show geochemical anomalies with respect to normal MORB (Pearce, 1983). Even excluding Sr, K, Rb and Ba, which may have been mobile at any stage of the evolution of these rocks, only sample CP10 showed a pattern similar to normal MORB; most of the retrogressed eclogites and amphibolites showed variable enrichments for most of the more incompatible elements. These compositions resemble those of transitional- to E-type MORB. The two well-preserved eclogites (Fig. 6a) were characterized by strong enrichment in Th, Ce and P relative to Zr, and pronounced negative Ta and Nb anomalies. The latter feature is particularly important as it is indicative of crustal influence in the pre-metamorphic evolution of the protolith.

Isotope data

Sm/Nd whole-rock data of metabasic rocks

Seven whole-rock samples (two well-preserved eclogites, one retrogressed eclogite, two amphibolites and two migmatite gneisses from the Deep Freeze Range) were selected for Sm–Nd isotope analyses. The analytical results are shown in Table 5. No isochron relationships can be inferred from the five metabasites. Nevertheless, excluding the two well-preserved eclogites, the other three samples scatter along a line with a slope of ~700 Ma and $\varepsilon_{Nd(i)}$ of 6·7. Present-day $\varepsilon_{Nd(0)}$ ranges from strongly

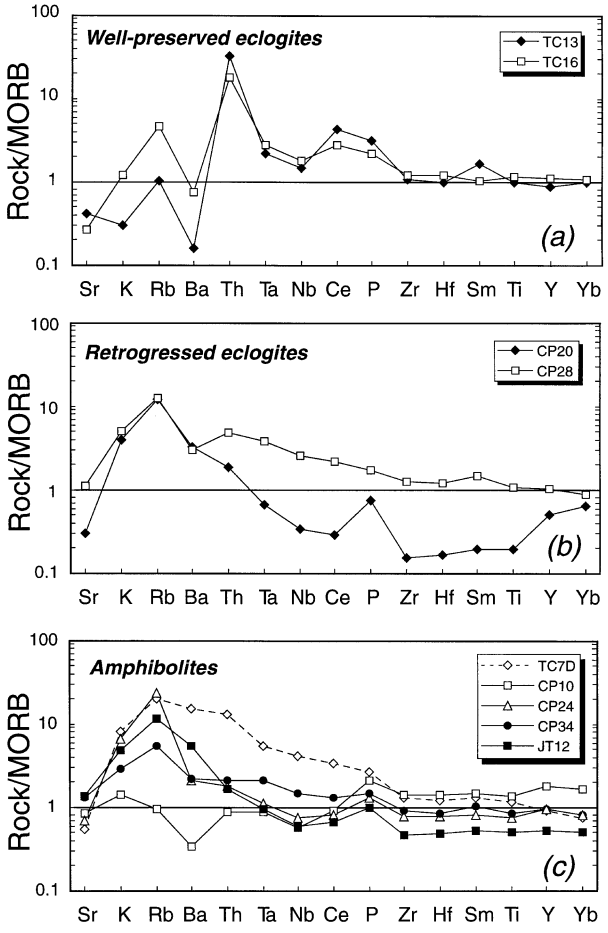

Fig. 6. MORB-normalized spidergrams for well-preserved eclogites (a), retrogressed eclogites (b) and amphibolites (c). Normalizing values are from Pearce (1983).

negative values for the two well-preserved eclogites (–7·0 and –7·4) to positive values for the other samples (from 4·0 to 11·3). Nd model ages (Table 5) relative to a linear depleted mantle evolution (Michard *et al.*, 1985) are around 1·5 Ga for the two well-preserved eclogites and between 0·50 and 0·93 Ga for the other samples. The two migmatite gneisses had exceedingly unradiogenic present-day composition and Nd model ages around 2·0 Ga (Table 5).

Sm/Nd and U/Pb data for minerals from well-preserved eclogites

Two well-preserved eclogites were selected for Sm–Nd isotope mineral analyses and for U–Pb analyses of rutile and whole rocks. One garnet fraction was also analysed for lead content and isotope compositions. The results are given in Tables 5 and 6. The garnet size (mostly ~0·3 mm) of the samples was too small to allow separation of different portions, so whole grains were analysed. In contrast to what we found with duplicate analysis of the whole rock, clinopyroxene and amphibole, the reproducibility of the $^{147}Sm/^{144}Nd$ and $^{143}Nd/^{144}Nd$ ratios of replicate garnet analyses was well outside analytical uncertainty. Although the very low Sm and Nd contents (~0·2 and ~0·1 p.p.m., respectively—Table 5) of the garnets make this phase susceptible to contamination by the other mineral phases (e.g. clinopyroxene, epidote and apatite) during mineral purification, significant zoning in the Sm and Nd contents of garnet is likely (Getty *et al.*, 1993; Brueckner *et al.*, 1996), especially if we take into account the occurrence of chemical zoning for major cations.

Figure 7a and b shows the Sm–Nd isotope data of whole rocks and minerals of samples TC13 and TC16 in isochron diagrams. For sample TC13, all mineral fractions and whole rock formed a well-defined isochron of age 500 ± 5 Ma [mean square weighted deviation (MSWD) = 1·13] with a $\varepsilon_{Nd(i)} = -3{\cdot}28 \pm 0{\cdot}14$ (Fig. 7a). No significant variation in age and initial ratio was observed when the amphibole data point was excluded from the regression calculation. Least-squares linear regression of all minerals and whole rock from sample TC16 (Fig. 7b) yielded an age of 491 ± 7 Ma (MSWD = 2·89) with $\varepsilon_{Nd(i)} = -3{\cdot}18 \pm 0{\cdot}31$. The MSWD of 2·89 indicates an excess of scattering according to the criterion of Wendt & Carl (1991). If the amphibole data are excluded from the calculation, we obtain a better fit corresponding to an age of 492 ± 3 Ma, $\varepsilon_{Nd(i)} = -3{\cdot}28 \pm 0{\cdot}14$ and an MSWD of 0·21.

Regarding the U–Pb data, in contrast to other results in pelitic systems (Mezger *et al.*, 1989*a*; Burton & O'Nions, 1991; Vance & O'Nions, 1992; Vance & Holland, 1993) no significant variations were observed between the Pb isotope ratios of the garnet and the respective whole rock (Table 6), making garnet in these rocks unsuitable for U–Pb age determination. In contrast to other documented findings [see Ludwig & Cooper (1984), Corfu & Muir (1989), Mezger *et al.* (1989*b*) or Tonarini *et al.* (1993) for mafic rocks], the rutile separates were characterized by low contents of radiogenic lead. Radiogenic Pb in the rutiles only accounted for ~10% and ~18% of total Pb in samples TC13 and TC16, respectively. Nevertheless, their U/Pb ratios were sufficiently higher than those of the whole rock, giving two-point isochrons with acceptable precision. The ^{235}U–^{207}Pb and ^{238}U–^{206}Pb two-point (rutile–whole-rock) ages of each sample were discordant, but the most reliable ^{238}U–^{206}Pb results (radiogenic ^{206}Pb was up to 19 × higher than radiogenic ^{207}Pb) yielded essentially identical ages of 495 ± 6 and 503 ± 6 Ma for TC13 and TC16, respectively (with a weighted mean of 499 ± 4 Ma). All four data points of the two samples scattered in a $^{206}Pb/^{204}Pb$ vs $^{238}U/^{204}Pb$ diagram along a line with an age of 502 ± 17 Ma (MSWD = 5·7). Hence we consider the ^{238}U–^{206}Pb ages to be the best

Table 5: Sm–Nd analytical results

Sample	Sm (p.p.m.)	Nd (p.p.m.)	$^{147}Sm/^{144}Nd$	$^{143}Nd/^{144}Nd$	$\pm 2\sigma_m$	$\varepsilon_{Nd(0)}$	$T_{(DM)}$ (Ga)
Well-preserved eclogites							
TC13 Rt	0·5843	2·637	0·1339	0·512271	±8	−7·2	
TC13 Cpx	3·016	12·91	0·1413	0·512284	±6	−6·9	
TC13 Cpx/d	3·054	13·08	0·1412	0·512286	±6	−6·9	
TC13 Grt	0·2365	0·1312	1·091	0·515419	±37	54·2	
TC13 Grt/d	0·2371	0·1096	1·309	0·516080	±50	67·1	
TC13 Am	0·4374	1·550	0·1706	0·512383	±40	−5·0	
TC13 Am/d	—	—	—	0·512427	±39	−4·1	
TC13 WR	5·278	23·02	0·1386	0·512254	±40	−7·5	
TC13 WR/d	5·308	23·20	0·1386	0·512280	±6	−7·0	1·52
TC16 Rt	0·4456	2·091	0·1288	0·512243	±9	−7·7	
TC16 Cpx*	7·039	33·23	0·1281	0·512237	±6	−7·8	
TC16 Grt	0·2049	0·1186	1·045	0·515212	±74	50·2	
TC16 Grt/d	0·2014	0·1102	1·105	0·515384	±14	53·6	
TC16 Am	0·2382	0·7935	0·1812	0·512430	±11	−4·1	
TC16 Am/d	—	—	—	0·512390	±35	−4·9	
TC16 WR	3·284	14·76	0·1345	0·512258	±6	−7·4	1·49
Retrogressed eclogite							
CP28 WR	4·536	15·40	0·1781	0·512845	±7	4·0	0·50
Amphibolites							
CP10 WR	4·859	11·60	0·2531	0·513216	±6	11·3	0·93
CP34 WR	3·279	10·33	0·1918	0·512994	±7	6·9	0·61
Migmatitic) Gneisses (Deep Freeze Range)							
L11A WR	6·871	38·47	0·1080	0·511518	±6	−21·85	2·12
CF8 WR	7·488	42·10	0·1075	0·511637	±10	−19·53	1·96

Mineral symbols according to Kretz (1983). WR, whole rock; /d, full duplicate analysis. Epsilon notation was calculated with respect to a chondritic reservoir with present $^{147}Sm/^{144}Nd = 0·1967$ and $^{143}Nd/^{144}Nd = 0·512638$. The model ages were calculated assuming a linear depleted mantle evolution with present $^{147}Sm/^{144}Nd = 0·222$ and $^{143}Nd/^{144}Nd = 0·513114$ (Michard *et al.*, 1985).
*May be contaminated by epidote.

Table 6: U–Pb analytical results

Sample	U (p.p.m.)	Pb (p.p.m.)	$^{235}U/^{204}Pb$*	$^{238}U/^{204}Pb$*	$^{208}Pb/^{204}Pb$*	$^{207}Pb/^{204}Pb$*	$^{206}Pb/^{204}Pb$*
Well-preserved eclogites							
TC13 Rt	0·654	0·463	0·746	102·8	40·951	16·066	26·229
TC13 Grt	0·0632	—	—	—	38·965	15·675	18·655
TC13 WR	0·638	4·27	0·0710	9·79	40·394	15·683	18·808
TC16 Rt	1·23	0·476	1·51	208·2	40·440	16·702	34·948
TC16WR	0·377	1·40	0·133	18·3	42·305	15·728	19·537

Mineral symbols according to Kretz (1983). WR, whole rock.
*Corrected for blank and mass fractionation.

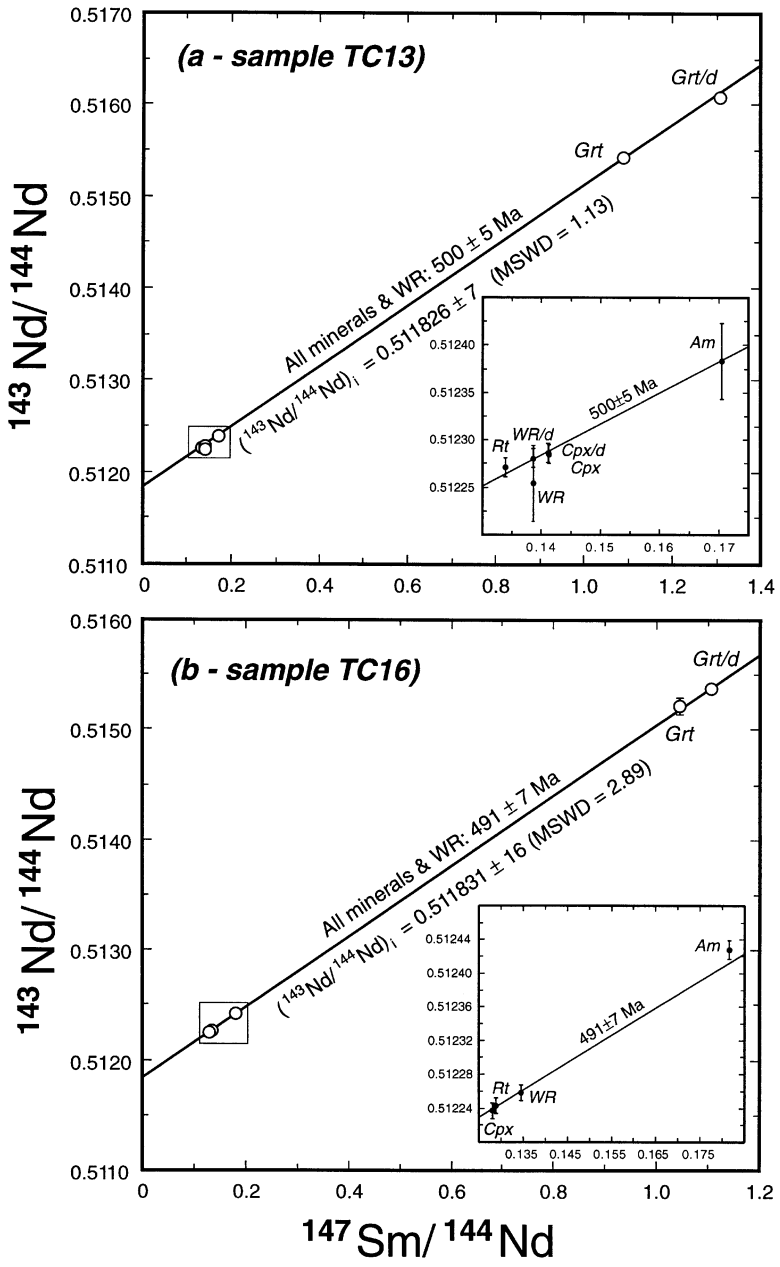

Fig. 7. Sm–Nd isochron diagram for the two well-preserved eclogite samples. Mineral symbols according to Kretz (1983). WR, whole rock. Excluding the amphibole data, we obtained an age of 500 ± 5 Ma (MSWD = 1·35) and 492 ± 3 Ma (MSWD = 0·21) for samples TC13 and TC16, respectively.

approximation of the age of cooling through the rutile closure temperature. It is noteworthy that these ages overlap the range of the Sm–Nd garnet ages. The ^{235}U–^{207}Pb ages of the two samples were younger and older than the ^{238}U–^{206}Pb age (~500 Ma), yielding ages of 456 ± 26 and 543 ± 23 Ma for TC13 and TC16, respectively.

DISCUSSION AND PETROGENESIS

Characteristics and age of the protoliths

Characterization of the geochemical affinity of ancient metabasic rocks can sometimes be difficult because the geochemical features may be the result of complex interplay between the magmatic evolution of the igneous

precursor and chemical modification promoted by recrystallization and deformational processes during metamorphism. For example, anomalous REE patterns for eclogite rocks have previously been described elsewhere (Griffin & Brueckner, 1985; Paquette *et al.*, 1989; Bernard-Griffiths *et al.*, 1991) and attributed to REE fractionation during metamorphism in a closed system (metamorphic layering) or in an open system with LREE loss (Bernard-Griffiths *et al.*, 1991). Except for the retrogressed eclogite CP20, such anomalous patterns were not observed among the samples analysed, and the consistency shown by high field strength elements (HFSE) and REE in most samples suggests that their distribution and contents may reflect the magmatic characteristics of the protoliths. As stated above, the amphibolites and retrogressed eclogites constituted a heterogeneous group with a compositional range from N-MORB to E-MORB. Moreover, the occurrence of Eu anomalies in some samples may indicate shallow-depth fractionation involving plagioclase.

Nd isotope data place further constraints on source compositions and the timing of these metabasites. Among the retrogressed eclogite and amphibolites, sample CP34 has an $^{147}Sm/^{144}Nd$ ratio of 0·192, close to that of chondrite, making its ε_{Nd} value practically insensitive to age correction. This means that sample CP34, with a present-day $\varepsilon_{Nd(0)}$ of 6·9, must be derived from a mantle source that was depleted for a substantial period of time.

As far as the age of these metabasites is concerned, unmetamorphosed mafic rocks older than the magmatic activity of the Ross Orogen are known from the Cotton Plateau (Nimrod Glacier area; Borg *et al.*, 1990) and from the Skelton Glacier area (Rowell *et al.*, 1993). Borg *et al.* (1990) reported an Sm–Nd three-point mineral–whole-rock isochron age of 762 ± 24 Ma for the gabbro and basalt of the Cotton Plateau with $\varepsilon_{Nd(i)} = 6{\cdot}85$. Rowell *et al.* (1993) inferred a maximum crystallization age of 700–800 Ma for the basalt of the Skelton Glaciers on the basis of Sm–Nd model ages. These mafic rocks were considered to be of oceanic type (Borg *et al.*, 1990) or continental rift affinity (Rowell *et al.*, 1993). Borsi *et al.* (1995) also described remnants of a mafic dyke swarm, recrystallized and metamorphosed during the Ross Orogeny, in the Deep Freeze Range (Wilson Terrane). They inferred an origin of the basaltic parental magma in a heterogeneous sub-continental lithosphere, and an emplacement age of 800–900 Ma.

Figure 8 shows an $\varepsilon_{Nd(0)}$ vs $^{147}Sm/^{144}Nd$ diagram of the analysed metabasites from the Lanterman Range and the data reported by Borg *et al.* (1990), Rowell *et al.* (1993) and Borsi *et al.* (1995). Figure 8 also includes two migmatite gneisses from the Deep Freeze Range (Wilson Terrane). The inset shows the Nd evolution for the samples relative to the reference reservoir (CHUR) compared with the Depleted Mantle and migmatite gneisses. The overlap of the two amphibolites and the retrogressed eclogite from the Lanterman Range (Fig. 8a) with the data reported by Borg *et al.* (1990) and Rowell *et al.* (1993) is noteworthy. All whole-rock samples, including the three samples from the Lanterman Range, scatter along a line with a slope of ~700 Ma and an $\varepsilon_{Nd(i)}$ of 6·8, whereas all 11 data points (including the plagioclase and the clinopyroxene separates from the gabbro of the Cotton Plateau and the three different concentrates from the basalt of the Skelton Glacier) yield an age of 725 ± 89 and an $\varepsilon_{Nd(i)}$ of 6·5. In addition, samples CP28 and CP10 define a line of age 754 ± 31 Ma and $\varepsilon_{Nd(i)} = 5{\cdot}9 \pm 0{\cdot}9$. This linear array of the samples on an isochron diagram is surprising because of their different geochemical signatures and the wide geographical distribution. If we consider that this correlation is not fortuitous, two alternative explanations are possible: (1) the correlation represents a mixing line or (2) it is geochronologically meaningful. The first possibility implies broad-scale mixing between a high ε_{Nd} and Sm/Nd component and a low ε_{Nd} and Sm/Nd end-member, and as a consequence, the linear array would indicate a maximum age. The second possibility requires that the retrogressed eclogite and amphibolite protoliths were derived from a mantle with a relatively uniform Nd isotope composition. In support of the latter interpretation is the fact that the ~700 Ma array is similar to the mineral–whole-rock age of the mafic rock of the Cotton Plateau (Borg *et al.*, 1990). The above arguments may therefore indicate that mafic magmatism with an affinity typical of a spreading setting and a depleted signature in terms of Nd isotope composition occurred in northern Victoria Land at ~700–750 Ma.

The two well-preserved eclogites are enriched in more incompatible elements and have high La/Ta and Th/Ta ratios that distinguish them from the amphibolites and retrogressed eclogites. The pronounced negative Ta and Nb anomalies of these rocks strongly suggest crustal influence of the pre-metamorphic magmatic evolution by intracrustal contamination or the effects of a metasomatized sub-continental lithosphere on the generation of the parental magma. In addition, the two well-preserved eclogites display unradiogenic Nd isotope composition and low $^{147}Sm/^{144}Nd$ ratios (Fig. 8). These compositions, along with trace element evidence, cannot be simply attributed to different emplacement ages but are the product of a magmatic process. Simple mixing of an igneous protolith with a depleted signature (similar to that of the retrogressed eclogites and amphibolites analysed) and a crustal component (similar in composition to the migmatite gneisses) at 700–750 Ma, would require a crustal contribution of at least 20% to account for the unradiogenic composition of the well-preserved eclogites. These samples, however, have low silica and relatively high MgO and transition element contents, not so compatible with crustal contamination *en route* of an igneous

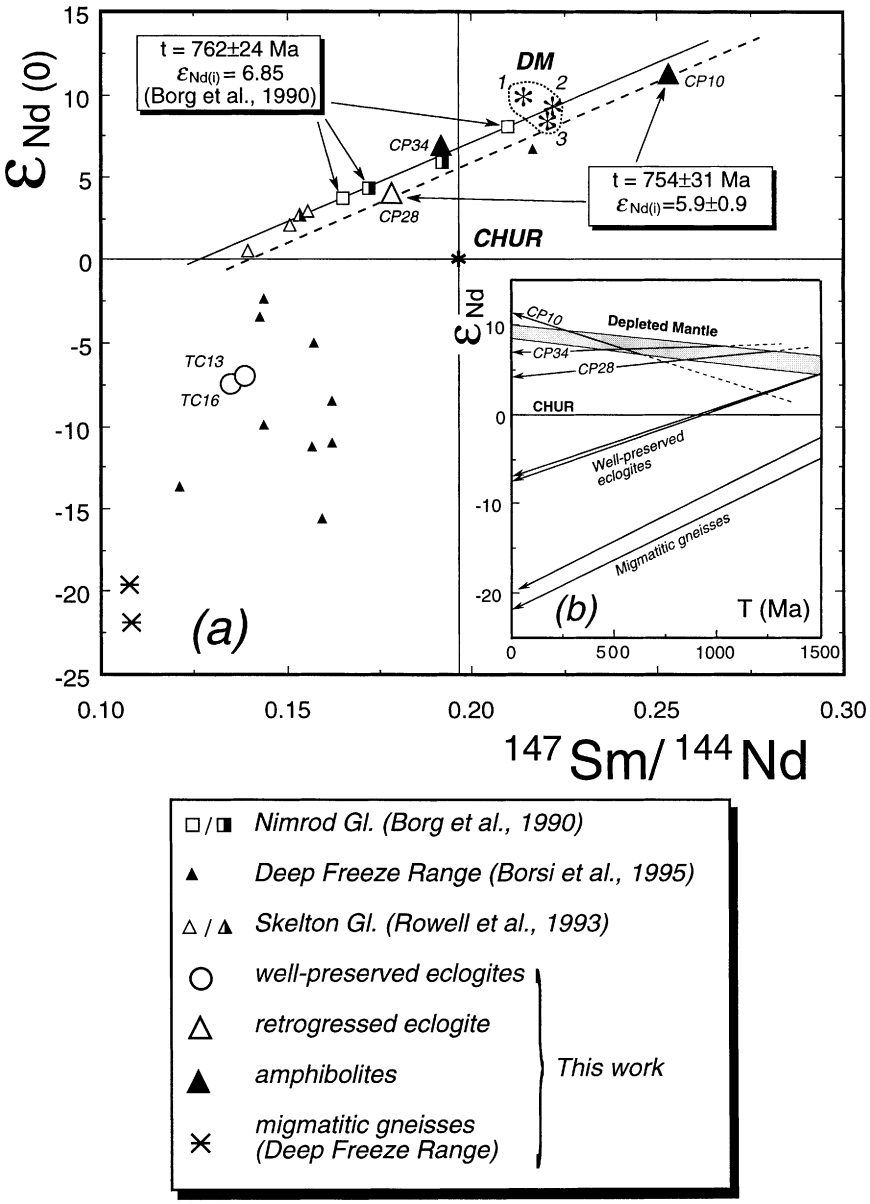

Fig. 8. $\varepsilon_{Nd(0)}$ vs $^{147}Sm/^{144}Nd$ diagram for the metabasites from Lanterman Range. Data for basic rocks from the Nimrod Glacier area (Borg *et al.*, 1990), Skelton Glacier area (Rowell *et al.*, 1993) and for metabasic rocks from the Deep Freeze Range (Borsi *et al.*, 1995) are plotted for comparison. Half-filled symbols refer to whole-rock data (see text). Depleted mantle compositions (DM) according to: (1) Goldstein *et al.* (1984); (2) Michard *et al.* (1985); (3) DePaolo (1981). The inset shows the Nd evolution of the analysed sample. The upper limit for the depleted mantle evolution curve is from Goldstein *et al.* (1984) and the lower limit from DePaolo (1981).

protolith similar in composition to the retrogressed eclogites and amphibolites. These arguments suggest that the well-preserved eclogites could be derived from a different mantle source with an enriched signature. Consequently, the ~1·5 Ga Nd model ages (Table 5) must be regarded as meaningless and not the true mantle separation age. The nature and time of the source enrichment as well as the age of the igneous precursor of the two well-preserved eclogites remain, at present, unconstrained. However, the evidence presented above indicates that along the suture between the Wilson Terrane and the allochthonous Bowers Terrane in the Lanterman Range,

different protoliths, possibly of different ages, may have experienced eclogite facies metamorphism.

Metamorphic evolution

The petrological data and mineral chemistry of eclogites from the Lanterman Range provide information on only the retrograde part of the P–T path of the rocks. The metamorphic evolution from the eclogite stage to the amphibolite facies retrogression, inferred from the petrological data and the experimentally determined reaction curves, is summarized by the P–T path in Fig. 9. The box of the eclogite facies stage is based on estimated temperatures and on the jadeite content of omphacite. The first post-eclogite stage (medium-pressure amphibolite facies stage) is documented both by the destabilization of omphacite, giving rise to the symplectitic association CpxII + Pl, and by the first appearance of amphibole (barroisite). Roermund & van Boland (1983) suggested that the degree of equilibration and the size of the retrometamorphic microstructures on omphacite are diffusion limited and temperature controlled. As the symplectite on omphacite is always cryptocrystalline, it presumably formed when the rocks were at relatively low temperatures. As the decompressional path after the eclogitic peak was therefore characterized by a decreasing temperature, any granulitic stage was excluded. The P–T box of this stage in Fig. 9 is based on estimated temperatures (630–750°C) and pressures (6–10 kbar). The subsequent low-pressure amphibolite facies stage characterized by the extensive development of tschermakitic hornblende is constrained by the experimental curves for amphibole (Plyusnina, 1982) and by the absence of chlorite (Fig. 9).

As far as the metamorphic evolution of the host-rocks is concerned, whether they were associated with mafic rocks during the high-pressure stage or had a different evolution is one of the most debated aspects of high-pressure terranes (Smith, 1988). In the Lanterman Range, field relationships such as lenses of quartzites and quartzo-feldspathic gneisses in large mafic bodies may reflect primary intrusive relations between the mafic rocks and part of the host-rocks. The petrographic data and P–T estimates in pelitic and quartz-feldspathic lithologies, however, contain no evidence of an eclogite stage. Nevertheless, the lack of high-pressure relics in pelitic and quartzo-feldspathic rocks is expected, as kinetic and equilibrium factors tend to preserve high-pressure mineralogy more in mafic rocks than in intermediate–felsic rocks (Koons & Thompson, 1985). However, the presence of relics of kyanite and phengite (Si^{4+} ~3·3 atoms per formula unit), and the microstructural features in the quartzo-feldspathic gneisses and garnet-bearing quartzites, in which garnet and phengite are surrounded by the symplectitic intergrowth consisting of biotite + plagioclase + quartz, are consistent (Godard, 1988) with a drop in pressure, and the reaction phengite + omphacite = biotite + plagioclase + quartz can be regarded as responsible for symplectite development on phengite. We therefore believe that the '*in situ* eclogite model', in which the metabasites and at least part of the host-rocks first underwent pervasive eclogite-facies metamorphism, is more likely for the Lanterman Range. Temperatures up to 850°C would even have generated melting in the KFMASH system of pelitic rocks under fluid-absent conditions (Le Breton & Thompson, 1988; Vielzeuf & Holloway, 1988). In quartzo-feldspathic rocks, because of the high thermal stability of the assemblage biotite + plagioclase + quartz at pressures >10 kbar, temperatures well above 850°C would have been required to produce melt (Vielzeuf & Montel, 1994). The absence of evidence of melting in the pelitic gneisses supports the interpretation that the mafic rocks could only have been associated with quartzites and quartzo-feldspathic rocks during the eclogite facies stage, whereas the pelitic gneisses were possibly juxtaposed at a later stage during exhumation of the high-pressure rocks. The estimated P–T conditions for the two amphibolite stages in the host-gneisses overlap the physical conditions of mafic rocks of the corresponding stages (Fig. 9). The formation of rare migmatites at Carnes Crags and Mt Bernstein is attributed to the medium- to low-pressure amphibolite stages.

In conclusion, the post-peak path of eclogites from the Lanterman Range is characterized by decreasing temperature and pressure, and overlaps the path of all the host-rocks from medium- to low-pressure amphibolite facies stage. As discussed by Koons & Thompson (1985), this path probably reflects rapid tectonic exhumation and would be appropriate to retain equilibration temperatures related to the depth of formation.

Significance of Sm/Nd and U/Pb mineral ages and age of the high-pressure metamorphism

In the last 10 years, many papers have demonstrated the potential of the Sm–Nd system to give high-precision ages in garnet-bearing metamorphic rocks [see Mezger *et al.* (1992) and references therein]. Garnet is also one of the main minerals used to establish P–T paths in medium- to high-grade metamorphic rocks, allowing direct correlation with age determinations. Nevertheless, large variations in the closure temperature (T_c) hypothesized for garnet, i.e. from ~600°C to ~900°C (Cohen *et al.*, 1988; Mezger *et al.*, 1992; Hensen & Zhou, 1995), require careful evaluation of whether garnet dating

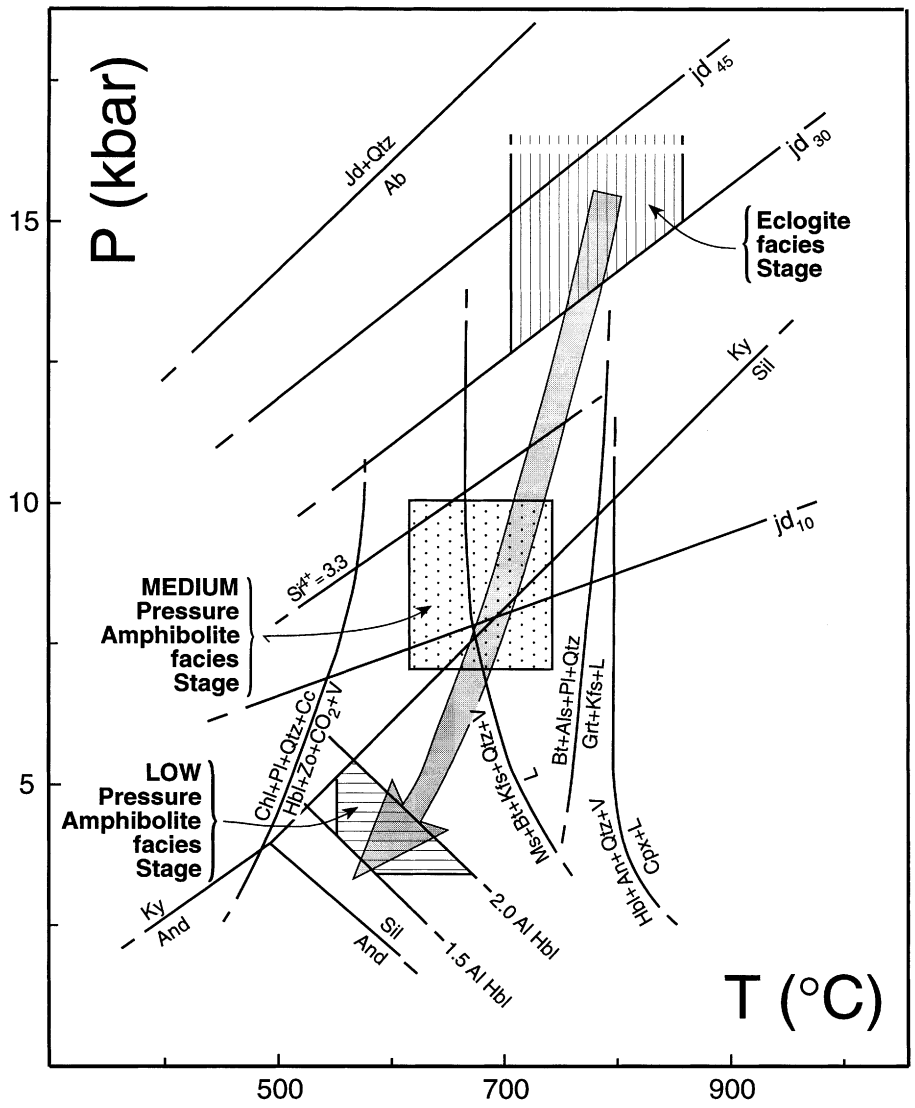

Fig. 9. *P–T* path (grey arrow) of the studied rocks. Aluminium silicate triple point is according to Holdaway (1971). Albite = jadeite + quartz and stability of omphacite (jd = 10, 30, 45) are after Holland (1983). Isopleth of Si^{4+} content in phengite barometer is after Massonne & Schreyer (1987). The curve representing the breakdown of amphibole is after Ellis & Thompson (1986). Chlorite + plagioclase + quartz + calcite = hornblende + zoisite + CO_2 + vapour and Al_{tot} content of hornblende are after Plyusnina (1982). Reactions in pelitic gneisses involving biotite and muscovite are according to Le Breton & Thompson (1988) and Vielzeuf & Holloway (1988), respectively. Mineral symbols are according to Kretz (1983).

represents the mineral growth or cooling age. This is particularly true for slow cooling terranes (1–5°C/m.y.), such as erosionally exhumed granulites, in which the Sm–Nd garnet age may considerably postdate mineral growth ages (Mezger *et al.*, 1992; Burton *et al.*, 1995). On the other hand, many papers on mafic eclogites have shown that, as the eclogite facies stage is usually followed by fast cooling, the Sm–Nd system on garnet records ages that are close to the high-pressure event (Griffin & Brueckner, 1985; Brueckner *et al.*, 1991; Becker, 1993; Miller & Thöni, 1995; Schmädicke *et al.*, 1995). Furthermore, Sm–Nd dates on high-pressure mafic rocks could be spurious where temperature was not high enough (see, e.g. Thöni & Jagoutz, 1992) or when the high-temperature stage was too short (see, e.g. Schmädicke *et al.*, 1995) for complete equilibration of garnet with the other mineral phases (mainly clinopyroxene). Garnet could also preserve zoned Sm–Nd

dates when the host-rock experienced multistage histories (Jamtveit *et al.*, 1991; Brueckner *et al.*, 1996) and, as a consequence, yield mixed ages if garnet is analysed as a whole.

As far as the present eclogites are concerned, the petrographic data do not indicate a polymetamorphic history, for which much more scatter would be expected between the garnet fractions of a single sample and/or between the internal isochrons of the two samples. Besides, incomplete isotopic equibilibration during the eclogitization process is not compatible with the good fit of the internal isochrons. The theoretical T_c (Dodson, 1979) can be calculated for garnet provided diffusion data for Sm and Nd and cooling rates are known. In our case, diffusion data for the Sm and Nd at temperatures relevant to the eclogite stage and independent estimates of the post-eclogitic cooling rate are not available. However, many workers [e.g. Chakraborty & Ganguly (1990) and Jamtveit *et al.* (1991)] agree that the diffusion parameters of Mg may represent the upper limit of the diffusion rate of Sm and Nd in garnet. Regarding the cooling rate, Goodge & Dallmeyer (1996) inferred a cooling rate as fast as 30°C/m.y. on the basis of $^{40}Ar/^{39}Ar$ mineral ages for metamorphic rocks of the southeastern Lanterman Range after the amphibolite facies metamorphism. This estimate may be a minimum value, as a higher cooling rate can be expected for the initial stage of cooling after the eclogite event. Assuming the self-diffusion data for Mg from the combined data set of Chakraborty & Ganguly (1990), spherical geometry and a cooling rate of 30°C/m.y., garnet diameters of 0·3 and 0·6 mm yield T_c of ~670°C and ~710°C, respectively. These temperatures can be regarded as the lower limit for Sm and Nd diffusion in garnet of the present eclogites.

As mentioned above, the two well-preserved eclogites yield essentially identical $^{238}U–^{206}Pb$ rutile–whole-rock ages of ~500 Ma that overlap the range of Sm–Nd garnet ages. Experimental diffusion data of U and Pb in rutile are not available, but comparison with other decay systems and/or different mineral ages strongly indicates that U–Pb ages of rutile reflect cooling below the T_c rather than mineral growth age (Mezger *et al.*, 1989*b*, 1991). On the basis of direct comparison between U–Pb ages of rutiles and K–Ar in hornblende and biotite in slow cooling terranes (0·5–1°C/m.y.), Mezger *et al.* (1989*b*) inferred a closure temperature of ~420°C for rutile with a radius of 0·09–0·21 mm. Assuming activation energies for U and Pb in rutile similar to those of Fe and Ti (in the range of 40–60 kcal/mol; Mezger *et al.*, 1989*b*), a cooling rate of 30°C/m.y. and the largest rutile grain size observed (up to ~0·2 mm), then the extrapolated T_c for rutile of the studied eclogites is around 500°C. The T_c calculated for garnet (670–710°C) and rutile (~500°C), and the overlap of the rutile and garnet ages strongly support a high initial cooling rate for the eclogites, even higher than the 30°C/m.y. estimated by Goodge & Dallmeyer (1996). If we also consider the petrographic observations and the P–T trajectory, fast cooling must have been accomplished by concomitant rapid exhumation.

The above arguments support the interpretation that the age of ~500 Ma obtained by the Sm–Nd method on garnet and the U–Pb method on rutile closely approaches the time of the eclogite facies metamorphism.

PALAEO-TECTONIC IMPLICATIONS

The eclogites of the Lanterman Range are the first reported record of a well-preserved high-pressure metamorphic event along the Antarctic palaeo-Pacific margin of Gondwana. Indeed, to our knowledge, the only evidence of eclogites in Antarctica, albeit cryptic, is from the Nimrod Group of the central Transantarctic Mountains (Goodge *et al.*, 1992). In the Tasmanian and eastern Australian segments of the palaeo-Pacific margin of Gondwana, mafic rocks preserving eclogite facies relics are known from the Tyennan region and the New England Fold Belt, respectively. The eclogites of Tasmania and eastern Australia show strong similarities with the new findings from Antarctica, as they have similar field characteristics (i.e. lenses in continental type metasediments and/or blocks in serpentinite melange) and P–T conditions of metamorphism (14–17 kbar, ~700°C). The Tasmanian eclogites (Franklin Metamorphics), previously considered Neoproterozoic (780 Ma; Raheim & Compston, 1977) were recently dated by SHRIMP and yielded a zircon age of ~500 Ma (Turner *et al.*, 1995). The age of the Australian eclogites was inferred to be Early Ordovician or, more likely, Cambrian (Watanabe *et al.*, 1993) from K–Ar age determinations on phengites from surrounding glaucophane schists.

The pre-orogenic setting

The pre-orogenic history of Lanterman metabasites is constrained by independent lines of evidence, including (1) the compositional features of the enclosing gneisses, (2) possible primary intrusive relations with part of the surrounding gneisses and (3) their geochemical compositions. As stated above, excluding the well-preserved eclogites, the retrogressed eclogites and amphibolites show a prevailing transitional- to E-type MORB affinity. Although the 'MORB' geochemical signature may be consistent with different geotectonic settings (open ocean, embryonic narrow ocean, back-arc basin), the geological relationships inferred between sill-like mafic intrusions, together with continental-type sediments and the predominance of samples with a transitional- to E-type MORB affinity are more consistent with an incipient

oceanic basin rather than a large, mature, oceanic domain. The age hypothesized for protolith formation of 'MORB-type' Lanterman metabasites (700–750 Ma) is similar to those of other mafic rocks with similar geochemical character scattered throughout the Transantarctic Mountains (Cotton Plateau, Skelton Glacier area). This evidence supports the view that diffuse mafic magmatism of spreading setting type occurred along the Pacific margin of eastern Gondwana during Neoproterozoic time. Nevertheless, the data do not clarify the meaning of the protoliths of the well-preserved eclogites and their tectonic setting.

The orogenic evolution

In stressing the particular structural position of the eclogites in the mafic–ultramafic belt at the eastern margin of the Wilson Terrane, Ricci *et al.* (1997*a*) proposed that the orogenic history of Lanterman eclogites could be wholly included in the Ross orogenic cycle. The data presented in this paper substantiate this scenario, especially the interpretation, supported by the mineralogical and compositional features of the eclogites, that the geochronological data closely approximate the age of the eclogite facies metamorphism. Additional arguments supporting a Ross-linkage for the formation and exhumation ages of the Lanterman eclogites arise from the reconstructed *P–T*–time path of eclogites in comparison with the metamorphic evolution recorded by other rock types from other localities in the eastern Wilson Terrane.

Broad complex zonation in terms of *P–T* regimes and partly contrasting post-peak *P–T*–time trajectories are significant features of the metamorphic pattern of the whole eastern margin of the Wilson Terrane [Ricci *et al.* (1996), fig. 3b, and references]. Specifically, cooling and unloading after a stage of moderate crustal thickening are recorded at Mt Murchison and in the north-eastern part of the Lanterman Range, and near-isothermal or slightly *T*-decreasing decompressional paths after a much deeper burial at Dessent Ridge and for the eclogites included in this study.

In summary, rocks units which recorded contrasting *P–T* metamorphic regimes and *P–T*–time path are juxtaposed in the same structural setting along the boundary between the Wilson Terrane and Bowers Terrane. The mafic rocks occurring along this boundary are heterogeneous in terms of geochemical affinity and possibly also in age of formation. All these considerations suggest that the Lanterman eclogites belong to a major structural zone which formed through tectonic imbrication of rock units from different domainal provenance, with different metamorphic evolution and a distinctive exhumation path. In this framework and on geochronological grounds, the most likely geotectonic setting for the formation and subsequent fast exhumation of eclogites is a convergent plate margin. These rocks consistently document the subduction–accretional nature of the early Palaeozoic Ross Orogen in northern Victoria Land (Kleinschmidt & Tessensohn, 1987; Borg & DePaolo, 1994). The chronological coincidence of the formation and exhumation of eclogite outboard the continental margin, and the generation and emplacement of calc-alkaline granitoids inboard the margin are consistent evidence that the Ross Orogen developed in the framework of a long-lasting subduction–accretion process which affected the Antarctic margin of Gondwana around 500 m.y. ago.

ACKNOWLEDGEMENTS

We thank G. Vaggelli for help with wavelength-dispersive spectrometry analyses, and S. G. Borg, C. Ghezzo and S. Tonarini for comments on an earlier version of the manuscript. G. D. expresses special thanks to R. J. Smeets and J. C. van Belle for assistance in the clean laboratory, and, in particular, to G. R. Davies and T. Elliott for invaluable suggestions on sample preparation for isotope analysis. The authors are indebted to M. Thirlwall for providing two NdO^+ isotope analyses on garnet used in this work. The manuscript was improved by thorough reviews by D. Ellis, D. Jacob-Foley and B. M. Jahn. This research was carried out with the financial support of the Italian 'Programma Nazionale di Ricerche in Antartide'.

REFERENCES

Ai Yang, 1994. A revision of the garnet–clinopyroxene Fe^{2+}–Mg exchange geothermometer. *Contributions to Mineralogy and Petrology* **115,** 467–473.

Armienti, P., Ghezzo, C., Innocenti, F., Manetti, P., Rocchi, S. & Tonarini, S., 1990. Isotope geochemistry of granitoid suites from Granite Harbour Intrusives of the Wilson Terrane, North Victoria Land, Antarctica. *European Journal of Mineralogy* **2,** 103–123.

Beccaluva, L., Ohnenstetter, D. & Ohnenstetter, M., 1979. Geochemical discrimination between ocean floor and island-arc tholeiites—application to some ophiolites. *Canadian Journal of Earth Sciences* **16,** 1874–1882.

Becker, H., 1993. Garnet peridotite and eclogite Sm–Nd mineral ages from Lepontine dome (Swiss Alps): new evidence from Eocene high-pressure metamorphism in the central Alps. *Geology* **21,** 599–602.

Bernard-Griffiths, J., Pecaut, J. J. & Ménot, R. P., 1991. Isotopic (Rb–Sr, U–Pb and Sm–Nd) and trace element geochemistry of eclogites from the pan-African Belt: a case study of REE fractionation during high-grade metamorphism. *Lithos* **27,** 43–57.

Borg, S. G. & DePaolo, D. J., 1994. Laurentia, Australia, and Antarctica as a late Proterozoic supercontinent: constraints from isotopic mapping. *Geology* **22,** 307–310.

Borg, S. G., DePaolo, D. J. & Smith, B., 1990. Isotopic structure and tectonics of the Central Transantarctic Mountains. *Journal of Geophysical Research* **95,** 6647–6667.

Borsi, L., Petrini, R., Talarico, F., & Palmeri, R., 1995. Geochemistry and Sr–Nd isotopes of amphibolite dykes of northern Victoria Land, Antarctica. *Lithos* **35,** 245–259.

Bradshaw, J. D. & Laird, M. G., 1983. The pre-Beacon geology of northern Victoria Land: a review. In: Oliver, R. H., James, P. R. & Jago, J. B. (eds) *Antarctic Earth Science*. Canberra, A.C.T.: Australian Academy of Sciences, pp. 98–101.

Brown, E. H., 1977. The crossite content of Ca-amphibole as a guide to pressure of metamorphism. *Journal of Petrology* **18,** 53–72.

Brueckner, H. K., Medaris, L. G. & Bakun-Czubarow, N., 1991. Nd and Sr age isotope patterns from Variscan eclogites of the eastern Bohemian Massif. *Neues Jahrbuch für Mineralogie, Abhandlungen* **163,** 169–196.

Brueckner, H. K., Blusztajn, J. & Bakun-Czubarow, N., 1996. Trace element and Sm–Nd 'age' zoning in garnets from peridotites of Caledonian and Variscan Mountains and tectonic implications. *Journal of Metamorphic Geology* **14,** 61–73.

Buggisch, W. & Kleinschmidt, G., 1989. Recovery and recrystallization of quartz and 'crystallinity' of illite in the Bowers and Robertson Bay Terranes (northern Victoria Land). In: Thompson, M. R. A., Crame, J. A. & Thompson, J. W. (eds) *Geological Evolution of Antarctica*. Cambridge University Press, pp. 155–160.

Burton, K. W. & O'Nions, R. K., 1991. High resolution garnet chronometry and the rates of metamorphic processes. *Earth and Planetary Science Letters* **107,** 649–671.

Burton, K. W., Kohn, M. J., Cohen, A. S. & O'Nions, R. K., 1995. The relative diffusion of Pb, Nd, Sr and O in garnet. *Earth and Planetary Science Letters* **133,** 199–211.

Capponi, G., Castelli, D., Fioretti, A. M. & Oggiano, G., 1995. Geological mapping and field relationships of the eclogites from the Lanterman Range (northern Victoria Land, Antarctica). *VII International Symposium on Antarctic Earth Sciences, Siena, 10–15 September, Abstracts. Siena: Terra Antarctica* p. 73.

Castelli, D., Lombardo, B., Oggiano, G., Rossetti, P. & Talarico, F., 1991. Granulite facies rocks of the Wilson Terrane (northern Victoria Land, Antarctica): Campbell Glacier. *Memorie della Società Geologica Italiana* **46,** 197–203.

Chakraborty, S. & Ganguly, J., 1990. Compositional zoning and cation diffusion in aluminosilicate garnets. In: Ganguly, J. (ed.) *Diffusion, Atomic Ordering and Mass Transfer, Advances in Physical Geochemistry, 8*. Berlin: Springer-Verlag, pp. 120–175.

Chavagnac, V. & Jahn, B. M., 1996. Coesite-bearing eclogites from the Bixiling Complex, Diabe Mountains, China: Sm–Nd ages, geochemical characteristics and tectonic implications. *Chemical Geology* **133,** 29–51.

Cohen, A. S., O'Nions, R. K., Siegenthaler, R. & Griffin, W. L., 1988. Chronology of the pressure–temperature history recorded by granulite terrain. *Contributions to Mineralogy and Petrology* **98,** 303–311.

Coleman, R. G., Beatty, L. B. & Brannock, W. W., 1965. Eclogites and eclogites: their differences and similarities. *Geological Society of America Bulletin* **76,** 483–508.

Corfu, F. & Muir, T. L., 1989. The Hemlo–Heron Bay greenstone belt and Hemlo Au–Mo deposit, Superior Province, Ontario, Canada. 2. Timing of metamorphism, alteration and Au mineralization from titanite, rutile, and monazite U–Pb geochronology. *Chemical Geology (Isotope Geosciences Section)* **79,** 201–223.

DePaolo, D. J., 1981. A neodymium and strontium isotope study of the Mesozoic calc-alkaline granitic batholiths of the Sierra Nevada and Peninsular Ranges, California. *Journal of Geophysical Research* **86,** 10470–10488.

Dodson, M. H., 1979. Theory of cooling ages. In: Jäger, E. & Hunziger, J. (eds) *Lectures in Isotope Geology*. Berlin: Springer-Verlag, pp. 194–202.

Ellis, D. J. & Green, D. H., 1979. An experimental study of the effect of Ca upon garnet–clinopyroxene Fe–Mg exchange equilibria. *Contributions to Mineralogy and Petrology* **71,** 13–22.

Ellis, D. J. & Thompson, A. B., 1986. Subsolidus and partial melting reactions in the quartz-excess $CaO + MgO + Al_2O_3 + SiO_2 + H_2O$ system under water-excess and water-deficient conditions to 10 kbar: some implications for the origin of peraluminous melts from mafic rocks. *Journal of Petrology* **27,** 91–121.

Essene, E. J. & Fyfe, W. S., 1967. Omphacite in California metamorphic rocks. *Contributions to Mineralogy and Petrology* **15,** 1–23.

Ferry, J. M. & Spear, F. S., 1978. Experimental calibration of the partitioning of Fe and Mg between biotite and garnet. *Contributions to Mineralogy and Petrology* **66,** 113–117.

Gebauer, D., 1990. Isotopic system–geochronology of eclogites. In: Carswell, D. A. (ed.) *Eclogite Facies Rocks*. Glasgow: Blackie, pp. 141–160.

Getty, S. R., Selverstone, J., Wernicke, B. P., Jacobsen, S. B., Aliberti, E. Lux, D. R., 1993. Sm–Nd dating of multiple garnet growth events in an arc–continent collision zone, northwestern U.S. Cordillera. *Contributions to Mineralogy and Petrology* **115,** 45–57.

Ghent, E. D. & Stout, M. Z., 1981. Geobarometry and geothermometry of plagioclase–biotite–garnet–muscovite assemblages. *Contributions to Mineralogy and Petrology* **76,** 92–97.

Godard, G., 1988. Petrology of some eclogites in the Hercynides: the eclogites from the southern Armorican Massif, France. In: Smith D. C. (ed.) *Eclogites and Eclogite-facies Rocks*. Amsterdam: Elsevier, pp. 451–510.

Goldstein, R. K., O'Nions, R. K. & Hamilton, P. J., 1984. A Sm–Nd isotopic study of atmospheric dusts and particulates from major river systems. *Earth and Planetary Science Letters* **70,** 221–236.

Goodge, J. W. & Dallmeyer, R. D., 1996. Contrasting thermal evolution within the Ross Orogen, Antarctica: evidence from mineral $^{40}Ar/^{39}Ar$ ages. *Journal of Geology* **104,** 435–458.

Goodge, J. W., Hansen, V. L. & Peacock, S. M., 1992. Multiple petrotectonic events in high-grade metamorphic rocks of the Nimrod Group, central Transantarctic Mountains, Antarctica. In: Yoshida, Y., Kaminuma, K. & Shiraishi, K. (eds) *Recent Progress in Antarctic Earth Science*. Tokyo: Terrapub, pp. 203–209.

Graham, C. M. & Powell, R., 1984. A garnet–hornblende geothermometer: calibration testing and application to the Pelona schist, southern California. *Journal of Metamorphic Geology* **2,** 13–31.

Grew, E. S., Kleinschmidt, G. & Schubert, W., 1984. Contrasting metamorphic belts in north Victoria Land. *Geologisches Jahrbuch* **B60,** 253–263.

Griffin, W. L. & Brueckner, H. K., 1985. REE, Rb–Sr and Sm–Nd studies of Norwegian eclogites. *Chemical Geology (Isotope Geosciences Section)* **52,** 249–271.

Hebeda, E. H., Andriessen, P. A. M. & van Belle, J. C., 1988. Simultaneous isotope dilution analysis of Sm and Nd with fixed multicollector mass spectrometer. *Fresenius' Zeitschrift für Analytische Chemie* **331,** 114–117.

Hensen, B. J. & Zhou, B., 1995. Retention of isotopic memory in garnets partially broken down during an overprinting granulite-facies metamorphism: implication for the Sm–Nd closure temperature. *Geology* **23,** 225–228.

Holdaway, M. J., 1971. Stability of andalusite and the aluminium silicate phase diagram. *American Journal of Science* **271,** 97–131.

Holland, T. J. B., 1983. The experimental determination of activities in disordered and short-range ordered jadeitic pyroxenes. *Contributions to Mineralogy and Petrology* **82,** 214–220.

Indares, A. & Martignole, J., 1985. Biotite–garnet geothermometry in the granulite facies: the influence of Ti and Al in biotite. *American Mineralogist* **70,** 272–278.

Jamtveit, B., Carswell, D. A. & Mearns, E. W., 1991. Chronology of the high-pressure metamorphism of Norwegian garnet peridotites/pyroxenites. *Journal of Metamorphic Geology* **9,** 125–139.

Kalt, A., Hanel, M., Schleicher, H. & Kramm, U., 1994. Petrology and geochronology of eclogites from the Variscan Schwarzwald (F.R.G.). *Contributions to Mineralogy and Petrology* **115,** 287–302.

Kleinschmidt, G. & Tessensohn, F., 1987. Early Paleozoic westward directed subduction of the Pacific margin of Antarctica. In: McKenzie, G. D. (ed.) *Gondwana Six: Structure, Tectonics, and Geophysics. Geophysical Monograph, American Geophysical Union* **40,** 89–105.

Kleinschmidt, G., Schubert, W., Olesch, M. & Rettmann, E. S., 1987. Ultramafic rocks of the Lanterman Range in north Victoria Land, Antarctica: petrology, geochemistry and geodynamic implications. *Geologisches Jahrbuch* **B66,** 231–273.

Koons, P. O. & Thompson, A. B., 1985. Non-mafic rocks in the greenschist, blueschist and eclogite facies. *Chemical Geology* **50,** 3–30.

Kretz, R., 1983. Symbols for rock-forming minerals. *American Mineralogist* **68,** 277–279.

Kreuzer, H., Hohndorf, A., Lenz, H., Muller, P. & Vetter, U., 1987. Radiometric ages of pre-Mesozoic rocks from northern Victoria Land, Antarctica. In: McKenzie, G. D. (ed.) *Gondwana Six: Structure, Tectonics, and Geophysics. Geophysical Monograph, American Geophysical Union* **40,** 31–47.

Krogh, E. J., 1988. The garnet–clinopyroxene Fe–Mg geothermometer—a reinterpretation of existing experimental data. *Contributions to Mineralogy and Petrology* **99,** 44–48.

Leake, B. E., 1978. Nomenclature of amphiboles. *American Mineralogist* **63,** 1023–1052.

Le Breton, N. & Thompson, A. B., 1988. Fluid-absent (dehydration) melting of biotite in metapelites in the early stages of crustal anatexis. *Contributions to Mineralogy and Petrology* **99,** 226–237.

Ludwig, K. R., 1990. ISOPLOT: a plotting and regression program for radiogenic isotope data, for IBM-PC compatible computers, Version 2.02. *US Geological Survey, Open-File Report* **88-557**.

Ludwig, K. R. & Cooper, J. A., 1984. Geochronology of Precambrian granites and associated U–Ti–Th mineralization, northern Olary province, South Australia. *Contributions to Mineralogy and Petrology* **86,** 298–308.

Marchand, J., 1974. Persistence d'une série granulitique au coeur du Massif central français (Haut Allier). Les termes acides. Thèse 3 cycle, University of Nantes, 207 pp.

Massonne, H. J. & Schreyer, W., 1987. Phengite geobarometry based on the limiting assemblage with K-feldspar, phlogopite, and quartz. *Contributions to Mineralogy and Petrology* **96,** 212–224.

Meschede, M., 1986. A method of discriminating between different types of mid-ocean ridge basalts and continental tholeiites with Nb–Zr–Y diagram. *Chemical Geology* **56,** 207–218.

Mezger, K., Hanson, G. N. & Bohlen, S. R., 1989*a*. U–Pb systematics of garnet: dating of growth of garnet in the Late Archean Pikwitonei granulite domain at Cauchon and Natawahunan Lakes, Canada. *Contributions to Mineralogy and Petrology* **101,** 136–148.

Mezger, K., Hanson, G. N. & Bohlen, S. R., 1989*b*. High precision U–Pb ages of metamorphic rutile: application to the cooling history of high-grade terranes. *Earth and Planetary Science Letters* **96,** 106–118.

Mezger, K., Rawnsley, C. M., Bohlen, S. R. & Hanson, G. N., 1991. U–Pb garnet, sphene, monazite and rutile ages: implications for the duration of high-grade metamorphism and cooling histories, Adirondacks Mts, New York. *Journal of Geology* **99,** 415–428.

Mezger, K., Essene, E. J. & Halliday, A. N., 1992. Closure temperatures of the Sm–Nd system in metamorphic garnets. *Earth and Planetary Science Letters* **113,** 397–409.

Michard, A., Gurriet, M., Soudant, M. & Albarede, F., 1985. Nd isotopes in French Phanerozoic shales: external vs internal aspects of crustal evolution. *Geochimica et Cosmochimica Acta* **49,** 601–610.

Miller, C. & Thöni, M., 1995. Origin of eclogites from the Austroalpine Öztal basement (Tyrol, Austria): geochemistry and Sm–Nd vs Rb–Sr isotope systematics. *Chemical Geology (Isotope Geosciences Section)* **122,** 199–225.

Mullen, E. D., 1983. $MnO/TiO_2/P_2O_5$: a minor element discriminant for basaltic rocks of oceanic environments and its implications for petrogenesis. *Earth and Planetary Science Letters* **62,** 53–62.

Newton, R. C. & Haselton, H. T., 1981. Thermodynamics of the garnet plagioclase–Al_2SiO_5–quartz geobarometer. In: Newton, R. C., Navrotsky, A. & Wood. B. J. (eds) *Thermodynamics of Minerals and Melts. Advances in Geochemistry, 1*. Berlin: Springer-Verlag, pp. 129–145.

Newton, R. C. & Perkins, D., 1982. Thermodynamic calibration of geobarometers based on the assemblages garnet–plagioclase–orthopyroxene–(clinopyroxene)–quartz. *American Mineralogist* **67,** 203–222.

Palmeri, R., Pertusati, P. C., Ricci, C. A. & Talarico, F., 1994. Late Proterozoic (?)–early Paleozoic evolution of the active Pacific margin of Gondwana: evidence from the southern Wilson Terrane (northern Victoria Land, Antarctica). *Terra Antartica* **1,** 5–9.

Paquette, J. L., Menot, R. P. & Peucat, J. J., 1989. REE, Sm–Nd and U–Pb zircon study of eclogites from the Alpine External Massifs (Western Alps): evidence for crustal contamination. *Earth and Planetary Science Letters* **96,** 181–198.

Pearce, J. A., 1975. Basalt geochemistry used to investigate past tectonic environment on Cyprus. *Tectonophysics* **25,** 41–67.

Pearce, J. A., 1982. Trace element characteristics of lavas from destructive plate boundaries. In: Thorpe, R. S. (ed.) *Andesite: Orogenic Andesites and Related Rocks*. Chichester, UK: John Wiley, pp. 525–548.

Pearce, J. A., 1983. Role of sub-continental lithosphere in magma genesis at active continental margins. In: Hawkesworth, C. J. & Norry, M. J. (eds) *Continental Basalts and Mantle Xenoliths*. Nantwich, UK: Shiva, pp. 209–229.

Pearce, J. A. & Cann, J. R., 1973. Tectonic setting of basic volcanic rocks determined using trace element analysis. *Earth and Planetary Science Letters* **19,** 290–300.

Pearce, J. A. & Norry, M. J., 1979. Petrogenetic implications of Ti, Zr, Y and Nb variation in volcanic rocks. *Contributions to Mineralogy and Petrology* **69,** 33–47.

Perchuck, L. L., Aranovich, L. Y. A., Podleskii, K. K., Lavrent'eva, I. V., Gerasimov, V. Y., Kitsul, V. I., Karsakov, L. P. & Berokinov, N. V., 1985. Precambrian granulites of the shields, eastern Siberia, USSR. *Journal of Metamorphic Geology* **3,** 265–310.

Plyusnina, L. P., 1982. Geothermometry and geobarometry of plagioclase–hornblende-bearing assemblages. *Contributions to Mineralogy and Petrology* **80,** 140–146.

Powell, R., 1985. Regression diagnostic and robust regression in geothermometer/geobarometer calibration: the garnet–clinopyroxene geothermometer revisited. *Journal of Metamorphic Geology* **3,** 327–342.

Raheim, A. & Compston, W., 1977. Correlation between metamorphic events and Rb–Sr ages in metasediments and eclogites from western Tasmania. *Lithos* **10,** 271–289.

Ricci, C. A., Talarico, F. & Palmeri, R., 1997*a*. Tectonothermal evolution of the Antarctic palaeo-Pacific active margin of Gondwana: a northern Victoria Land perspective. In: Ricci, C. A. (ed.) The Antarctic Region: Geological Evolution and Processes. Siena: *Terra Antarctica special issue,* in press.

Ricci, C. A. & Tessensohn, F., 1997*b*. The Lanterman–Mariner suture. Antarctic evidence for Paleozoic active margin of Gondwana. *Geologisches Jahrbuch*, in press.

Ricci, C. A., Talarico, F., Palmeri, R., Di Vincenzo, G. & Pertusati, P. C., 1996. Eclogite at the Antarctic palaeo-Pacific margin of Gondwana (Lanterman Range, northern Victoria Land, Antarctica). *Antarctic Science* **8**(3), 277–280.

Roermund, H. L. M. & van Boland, J. N., 1983. Retrograde *P–T* trajectories of high temperature eclogites deduced from omphacite exsolution microstructures. *Bulletin Minéralogique* **106,** 723–726.

Roland, R. W., Gibson, G. M., Kleinschmidt, G. & Schubert, W., 1984. Metamorphism and structural relations of the Lanterman metamorphics, north Victoria Land, Antarctica. *Geologisches Jahrbuch* **B60,** 319–361.

Rowell, A. J., Rees, M. N., Duebendorfer, E. M., Wallin, E. T., van Schmus, W. R. & Smith, E. I., 1993. An active Neoproterozoic margin: evidence from the Skelton Glacier area, Transantarctic Mountains. *Journal of the Geological Society, London* **150,** 677–682.

Ryburn, R. J., Raheim, A. & Green, D. H., 1976. Determination of the *P–T* paths of natural eclogites during metamorphism, a record of subduction. A correction. *Lithos* **9,** 161–165.

Saunders, A. D., 1984. The rare earth element characteristics of igneous rocks from the ocean basins. In: Henderson, P. (ed.) *Rare Earth Element Geochemistry*. Amsterdam: Elsevier, pp. 205–236.

Schmädicke, E., Mezger, K., Cosca, M. A. & Okrusch, M., 1995. Variscan Sm–Nd and Ar–Ar ages of eclogite facies rocks from the Erzgebirge, Bohemian Massif. *Journal of Metamorphic Geology* **13,** 537–552.

Shervais, J. K., 1982. Ti–V plots and the petrogenesis of modern and ophiolitic lavas. *Earth and Planetary Science Letters* **59,** 101–118.

Smith, D. C., 1988. A review of the peculiar mineralogy of the 'Norwegian coesite–eclogite province', with crystal-chemical, petrological, geochemical and geodynamical notes and an extensive bibliography. In: Smith, D. C. (ed.) *Eclogites and Eclogite-facies Rocks*. Amsterdam: Elsevier, pp. 1–178.

Spear, F. S., 1980. NaSi–CaAl exchange equilibrium between plagioclase and amphiboles. An empirical model. *Contributions to Mineralogy and Petrology* **72,** 33–41.

Sun, S. S. & McDonough, W. F., 1989. Chemical and isotopic systematics of oceanic basalts: implications for mantle composition and processes. In: Saunders, A. D. & Norry, M. J. (eds) *Magmatism in the Ocean Basins. Geological Society, London, Special Publication* **42,** 315–345.

Talarico, F., Franceschelli, M., Lombardo, B., Palmeri, R., Pertusati, P. C., Rastelli, N. & Ricci, C. A., 1992. Metamorphic facies of the Ross Orogeny in the southern Wilson Terrane of northern Victoria Land, Antarctica. In: Yoshida, Y., Kaminuma, K. & Shiraishi, K. (eds.) *Recent Progress in Antarctic Earth Science*. Tokyo: Terrapub, pp. 211–218.

Thirlwall, M. F., 1991. High-precision multicollector isotopic analysis of low levels of Nd as oxide. *Chemical Geology* **94,** 13–22.

Thöni, M. & Jagoutz, E., 1992. Some new aspects of dating eclogites in orogenic belts: Sm–Nd, Rb–Sr and Pb–Pb isotopic results from the Austroalpine Saualpe and Koralpe type-locality (Carinthia/Styria, southern Austria). *Geochimica et Cosmochimica Acta* **56,** 347–368.

Tonarini, S., Villa, I. M., Oberli, F., Meier, M., Spencer, D. A., Pognante, U. & Ramsay, J. G., 1993. Eocene age of eclogite metamorphism in Pakistan Himalaya: implications for India–Eurasia collision. *Terra Nova* **5,** 13–20.

Turner, N. J., Black, L. P. & Kamperman, M., 1995. Pre-middle Cambrian stratigraphy, orogenesis and geochronology in western Tasmania. *Geological Society of Australia, Tasmanian Division, Contentious Issues in Tasmanian Geology: a Symposium*, pp. 51–56.

Ungaretti, L., Smith, D. C. & Rossi, G., 1981. Crystal-chemistry by X-ray structure refinement and electron microprobe analysis of a series of sodic–calcic to alkali-amphiboles from the Nybo eclogite pod, Norway. *Bulletin Minéralogique* **104,** 400–412.

Vance, D. & Holland, T., 1993. A detailed isotopic and petrological study of a single garnet from the Gassets Schist, Vermont. *Contributions to Mineralogy and Petrology* **114,** 101–118.

Vance, D. & O'Nions, R. K., 1992. Prograde and retrograde thermal histories from the central Swiss Alps. *Earth and Planetary Science Letters* **114,** 113–129.

Vidal, P. & Hunziker, J. C., 1985. Systematics and problems in isotope work on eclogites. *Chemical Geology (Isotope Geosciences Section)* **52,** 129–141.

Vielzeuf, D. & Holloway, J. R., 1988. Experimental determination of the fluid-absent melting relations in the pelitic system. *Contributions to Mineralogy and Petrology* **98,** 257–276.

Vielzuef, D. & Montel, J. M., 1994. Partial melting of metagreywackes. Part I. Fluid-absent experiments and phase relationships. *Contributions to Mineralogy and Petrology* **117,** 375–393.

Watanabe, T., Leicht, E. C., Itaya, T. & Fukui, S., 1993. Eclogite and glaucophane schist from eastern Australia: evidence for early Paleozoic convergence at eastern Gondwana margin. Fourth International Eclogite Conference, Cosenza 6–9 September, *Terra Abstract* **4**, supplement to *Terra Nova* **5,** 28.

Weaver, S. D., Bradshaw, J. D. & Laird, M. G., 1984. Geochemistry of Cambrian volcanics of the Bowers Supergroup and implications for the early Paleozoic tectonic evolution of northern Victoria Land, Antarctica. *Earth and Planetary Science Letters* **68,** 128–140.

Wendt, I. & Carl, C., 1991. The statistical distribution of the mean squared weighted deviation. *Chemical Geology (Isotope Geosciences Section)* **86,** 275–285.

Wood, D. A., Joron, J. L. & Treuil, M., 1979. A re-appraisal of the use of trace elements to classify and discriminate between magma series erupted in different tectonic settings. *Earth and Planetary Science Letters* **45,** 326–336.

APPENDIX: ANALYTICAL TECHNIQUES

Mineral analyses were performed on a JEOL JX 8600 electron microprobe fitted with four wavelength-dispersive spectrometers at the Department of Earth Sciences of Florence. Accelerating voltage was 15 kV and sample current 10 nA. Natural standards were used for calibration.

Major and trace elements were determined by inductively coupled plasma (ICP)-emission spectrometry (major elements and Sc) and ICP-mass spectrometry at the CRPG (Vandœuvre-les-Nancy, France), except for K_2O and loss on ignition, which were determined at the Department of Earth Sciences of Siena by atomic absorption spectrometry and by gravimetry at 1000°C after pre-heating at 110°C, respectively.

Mineral and chemical separation was achieved at the Faculteit der Aardwetenschappen of the Vrije Universiteit of Amsterdam. Minerals were concentrated from the grain size fraction of 63–125 μm using a Frantz Isodynamic separator and heavy liquids, and were carefully purified by handpicking under a binocular microscope, cleaned ultrasonically and dried with ultrapure acetone. All mineral separates were washed in warm 2N HCl for about 30 min. Whole rocks and rutile were digested in PTF Teflon bombs at 220°C using a mixture of concentrated HF and HNO_3. All the other mineral

separates were digested with a mixture of concentrated HF and HNO_3 in screw-top PFA Teflon beakers on a hot plate. Two separate aliquots were spiked with mixed ^{150}Sm–^{148}Nd and ^{235}U–^{208}Pb spikes, respectively. Single ^{235}U and ^{208}Pb spikes were used for whole rocks. The REE were separated as a group using TRU-SPEC (medium) chromatographic extraction material and 2N HNO_3 as eluant, whereas Sm and Nd were separated by HDEHP Teflon columns. Pb was separated by HCl–HBr chemistry using AG1x8 (200–400 mesh) anion exchange resins. U was separated using U-TEVA SPEC (medium) chromatographic extraction material and 2N HNO_3 as eluant. Sample weights were in the 0·2–0·5 g range for rutile, clinopyroxene, amphibole and whole rock, and 1·3–1·5 g and ~0·5 g for garnet in the Sm–Nd and U–Pb determinations, respectively. Sm and Nd blanks were <50 pg and <100 pg for garnet, and <20 pg and <50 pg for the other minerals or the whole rocks, respectively. Pb blanks were 100 pg for whole rocks and ≤300 pg for rutile and garnet. U blank was <50 pg.

All isotope analyses except for two garnet Nd isotope compositions (Grt/d, Table 5) that were run as NdO^+ at the Department of Geology, Royal Holloway University of London, following the procedure of Thirlwall (1991), were performed at the Faculteit der Aardwetenschappen of the Vrije Universiteit of Amsterdam. Mass spectometry analyses were performed with a Finnigan Mat 261 multicollector mass spectrometer. Nd was run as metal and the isotope ratios were normalized to $^{146}Nd/^{144}Nd = 0{\cdot}7219$. During the course of this study La Jolla Nd standard gave an average of $0{\cdot}511848 \pm 8$ (2σ, $n = 6$). For all isochron calculations a minimum uncertainty of $\pm 0{\cdot}002\%$ (2σ) was assumed for isotope compositions. Sm and Nd concentrations were determined following the procedure of Hebeda *et al.* (1988). The uncertainty for the Sm/Nd ratio was taken to be $\pm 0{\cdot}4\%$. The Sm/Nd ratio for rock standard BHVO-1 was 0·2472 (Sm = 6·121 p.p.m., Nd = 24·76 p.p.m.). All measured Pb isotope ratios were corrected with a mass fractionation factor of $0{\cdot}14 \pm 0{\cdot}01\%$ per mass unit based on repeated analyses of the NBS SRM 981 Pb standard, and for blank contribution. The blank correction was insignificant for whole-rock data. Reproducibility of the $^{208}Pb/^{204}Pb$, $^{207}Pb/^{204}Pb$ and $^{206}Pb/^{204}Pb$ ratios for the standard was within 0·12% (2σ), 0·02% (2σ) for the $^{207}Pb/^{206}Pb$ ratio and 0·03% (2σ) for the $^{208}Pb/^{206}Pb$ ratio, and was assumed as minimum uncertainty for age calculations. U was run with an electron multiplier and corrected with a mass fractionation factor of 0·21% per mass unit based on repeated analyses of the U500 standard. The estimated error on U/Pb ratios was less than $\pm 1\%$.

Isochron calculations were performed using the ISOPLOT program of Ludwig (1990).